

A search for hidden white dwarfs in the *ROSAT* EUV survey[†]

M. R. Burleigh^{1*}, M. A. Barstow^{1*} and T. A. Fleming²

¹ *Department of Physics and Astronomy, University of Leicester, University Rd., Leicester, LE1 7RH*

² *Steward Observatory, University of Arizona, Tucson, Arizona 85721, USA*

[†] *Based on observations made with the ROSAT observatory and the International Ultraviolet Explorer (IUE) satellite*

**Guest Observers with the International Ultraviolet Explorer (IUE) satellite*

January 11th 1997

ABSTRACT

The *ROSAT* WFC survey has provided us with evidence for the existence of a previously unidentified sample of hot white dwarfs (WD) in non-interacting binary systems, through the detection of EUV and soft X-ray emission. These stars are hidden at optical wavelengths due to their close proximity to much more luminous main sequence (MS) companions (spectral type K or earlier). However, for companions of spectral type \sim A5 or later the white dwarfs are easily visible at far-UV wavelengths, and can be identified in spectra taken by *IUE*. Eleven white dwarf binary systems have previously been found in this way from *ROSAT*, *EUVE* and *IUE* observations (e.g. Barstow et al. 1994). In this paper we report the discovery of three more such systems through our programmes in recent episodes of *IUE*. The new binaries are HD2133, RE J0357+283 (whose existence was predicted by Jeffries, Burleigh and Robb 1996), and BD+27°1888. In addition, we have independently identified a fourth new WD+MS binary, RE J1027+322, which has also been reported in the literature by Genova et al. (1995), bringing the total number of such systems discovered as a result of the EUV surveys to fifteen. We also discuss here six stars which were observed as part of the programme, but where no white dwarf companion was found. Four of these are coronally active. Finally, we present an analysis of the WD+K0IV binary HD18131 (Vennes et al. 1995), which includes the *ROSAT* PSPC X-ray data.

Key words: Stars: binaries – Stars: white dwarfs – X-ray: stars – Ultra-violet: stars.

1 INTRODUCTION

The extreme ultraviolet (EUV) surveys of the *ROSAT* Wide Field Camera (WFC, Pounds et al. 1993, Pye et al. 1995) and the Extreme Ultraviolet Explorer (*EUVE*, Bowyer et al. 1994, 1996) have found a substantial number of hot white dwarfs (\approx 120). The majority of these are single isolated stars, but about 30 are now known to lie in binary systems. Some have been identified because they are in interacting Cataclysmic Variable systems. Others have been found, from optical observations, to be in pairs with faint red dwarf companions (e.g. RE J1629+780, Cooke et al. 1992). A few are in wide, resolved binaries (e.g. HD74389B, Liebert, Bergeron and Saffer 1990). However, unresolved, non-interacting pairs with companions earlier than M-type have remained very difficult to identify.

In optical surveys, white dwarfs have been identified on the basis of colour information (e.g. Green, Schmidt and

Liebert 1986), and there is thus a selection effect against the detection of those in unresolved binaries. Any companion star of type K or earlier will completely dominate the optical spectrum of the white dwarf (see Figure 15). For example, Sirius B would be optically undetectable were it not for the close proximity of the system to Earth (2.64pc), allowing it to be resolved from Sirius A.

Several unresolved systems have been discovered serendipitously. The white dwarf in the well-studied system V471 Tauri was found as a result of an eclipse by its K2V companion (Nelson & Young 1970). A number of others have been found by chance in ultraviolet (UV) spectra taken by the International Ultraviolet Explorer (*IUE*). For example, the white dwarf companion to HD27483 (Böhm-Vitense 1993) was discovered as part of an *IUE* study of Hyades F stars by Böhm-Vitense (1995). Others detected in a similar fashion include ζ Cap (Böhm-Vitense 1980), 56 Peg (Schindler et al. 1982) and 4 σ^1 Ori (Johnson & Ake 1986).

In 1989, Shipman and Geczi conducted a systematic survey of the then existing *IUE* archive for white dwarf companions to G, K and M stars, but found no further examples.

Recently Landsman, Simon and Bergeron (1996) have detected, using *IUE*, two white dwarf companions to F stars showing an excess of ultraviolet radiation in the *TD-1* sky survey (Thompson et al. 1978). The white dwarf in the 56 Persei system (F4V) is, at $T=16,400\text{K}$, too cool to be seen with the WFC. The white dwarf companion to HR3643 is hot ($29,000 < T < 36,000$), but it is not detected by either *EUVE* or *ROSAT*. This is probably because of a high interstellar hydrogen column ($\sim 2 \times 10^{20} \text{cm}^{-2}$) to this star.

ROSAT and *EUVE* have now provided us with evidence for the existence of many more of these hidden hot white dwarfs through the detection of EUV and soft X-ray emission. Follow-up observations in the UV with *IUE* have enabled detection of unresolved white dwarfs in systems with a companion later than spectral type $\sim A5$. The initial discovery of companions to β Crateris (A2IV, Fleming et al. 1991) and HD33959C (KW Aur C, F4V, Hodgkin et al. 1993) was followed by seven others, all discussed in Barstow et al. (1994): BD+08°102 (K1-3V, also Kellett et al. 1995), HR1608 (K0IV, also Landsman, Simon, Bergeron 1993, hereafter LSB), HR8210 (IK Peg, A8m, also LSB, Wonnacott et al. 1993, Barstow, Holberg and Koester 1994), HD15638 (F3-6V, also LSB, Barstow, Holberg and Koester 1994), HD217411 (G5), HD223816 (F5-G0), and RE J1925–566 (G2-8). Since then Vennes et al. (1995) have reported a DA companion to the active K0IV star HD18131 through its detection as an *EUVE*/WFC source, and Christian et al. (1996) have discovered yet another DA+G star binary, MS 0354.6–3650, which is also an *EUVE* source (although it does not appear in the *ROSAT* WFC catalogues). This work has clearly demonstrated that there is an as yet unexplored population of white dwarfs with companions earlier than type M.

Most of these white dwarfs are all relatively bright EUV sources (with the exceptions of BD+08°102 and MS 0354.6–3650), with distinctive spectral signatures. Typically, the S2/S1 count rate ratios are >2 . For example HD33959C has a count rate of 2.628s^{-1} in the WFC S2 filter, and 1.172s^{-1} in S1. Comparisons with known white dwarfs detected by the WFC (e.g. GD659 2.193s^{-1} in S2, 0.722s^{-1} in S1) left little doubt that these sources were indeed white dwarfs. The observations with *IUE* merely confirmed the identifications.

About 120 of the 383 sources in the original Bright Source Catalogue (BSC, Pounds et al. 1993) have been associated with hot white dwarfs, and a larger number (~ 180) with active late type stars. However, from a cursory glance at the original BSC, it is clear that some of these late type stars were not previously known to be chromospherically active. Indeed, follow-up optical studies (e.g. Mason et al. 1995, Mullis and Bopp 1994) failed to find any evidence of activity at all in a few cases. It is also obvious from the WFC catalogues that there are many faint hot white dwarfs with low count rates, and with EUV colours that are not particularly distinctive. These stars may lie in relatively high column directions that affect the S2/S1 ratio and, from the count rates alone, it is difficult to immediately distinguish them from an active star. Furthermore, some of the primaries in the binaries already discovered are also active

(e.g. HD18131, BD+08°102 and RE J1925–566). Determining which EUV source is due to an active star and which is due to a white dwarf is clearly, in some cases, not an easy task. Given all these factors we continued to use *IUE* to search for further, less obvious white dwarfs hidden in non-interacting binaries. Since we began our *IUE* programmes the 2nd *ROSAT* WFC catalogue (Pye et al., 1995) has been published. This utilises improved source detection methods and contains 120 new sources as well as updating the BSC identifications. There is thus a pool of new, fainter and less obvious candidates requiring observation.

In this paper we report the results of our latest searches with *IUE*. We have identified four more hot white dwarfs in non-interacting binary systems with main sequence stars earlier than type M. They are HD2133 (RE J0024–741), RE J0357+283, BD+27°1888 (RE J1024+262) and RE J1027+322. Jeffries, Burleigh and Robb (1996) had previously predicted a hidden hot white dwarf as the most likely source of the EUV radiation in RE J0357+283. RE J1027+322 has also been independently reported by Genova et al. (1995); we present further observations and analysis of this system. This brings the total number of these WD+MS binaries discovered as a result of EUV surveys to fifteen.

We also provide in this paper an analysis of the white dwarf companion to HD18131, discovered and reported by Vennes et al. (1995). We include X-ray data from the *ROSAT* Position Sensitive Proportional Counter (PSPC), which were not available to Vennes et al. Those authors had observed Mg II emission lines in *IUE* LWP spectra of the K0IV primary, suggesting that it is active. We detect X-ray radiation from this system in the PSPC upper band which could not have come from the white dwarf, confirming that the K0IV star is indeed active.

In addition, we report here observations of six EUV sources where no white dwarf was found. Four of these ‘non-detections’ (BD–00°1462, CD–44 1025, HR1249 and HR2468) are active stars, and have been studied by others both in the UV and the optical. We summarise the properties and observations of these stars, and compare them with the binaries. We note that their UV spectra show evidence of activity (e.g. CIV and CII emission features) and compare the level of activity with other known active stars observed with the WFC. In two cases (AG+68 14, HD166435) there is no evidence of activity in the *IUE* spectra, and we find no reports in the literature of these being active stars. We therefore conclude that the counterparts to the EUV sources (2RE J0014+691 and RE J1809+295 respectively) may lie elsewhere in the fields of these stars and further observations are necessary.

The vast majority of the >1500 known white dwarfs are isolated stars. Theory suggests, however, that over half of all stars should be in binary or multiple systems. The presence of this new population of white dwarfs in binaries has profound implications, therefore, for our knowledge of the intrinsic white dwarf luminosity function, formation rate and space density, as determined by e.g. Fleming, Liebert and Green (1986). Observations of white dwarfs in binaries also allows us to place constraints on binary evolution models (e.g. de Kool and Ritter 1993).

2 OBSERVATIONS

2.1 Detection of the sources in the ROSAT and EUVE surveys

The ROSAT WFC EUV and X-ray all-sky surveys were conducted between July 1990 and January 1991; the mission and instruments are described elsewhere (Trümper 1992, Sims et al. 1990). The sources discussed in this paper are all listed in the original WFC Bright Source Catalogue (Pounds et al. 1993) and in the 2RE Catalogue (Pye et al. 1995). The revised catalogue contains 479 sources, as compared to 383 in the original survey. The complete survey database was reprocessed with improved methods for source detection, better background screening, etc., to give the 2RE Catalogue. The 2RE count rates are quoted in this paper. These are equivalent, on axis ‘at-launch’ values. The PSPC count rates for all the white dwarfs detected in the X-ray survey, including the binaries discussed here, are given in Fleming et al. (1996). The PSPC count rates for the active stars (i.e. the non-detections of white dwarf binaries) discussed in section 5.2 were obtained via the World Wide Web from the on-line ROSAT All-Sky Survey Bright Source Catalogue, maintained by the Max Planck Institute in Germany (Voges et al., 1997).

Some of the sources were also detected by EUVE in its all-sky survey (Bowyer et al. 1994, 1996). In Table 1 we list all the ROSAT and EUVE detections and count rates for our sources. The quoted EUVE count rates are from the Second EUVE Source Catalog (Bowyer et al. 1996), which includes an improved all-sky detection method offering better detection sensitivity and reliability.

2.2 Selection and Identification of White Dwarfs in Unresolved Binaries

The hot white dwarfs detected in the ROSAT EUV and X-ray all-sky surveys typically have very soft spectra compared to normal stars, particularly when the hydrogen column is low. The ratio of the WFC survey S2 to S1 count rates can sometimes exceed a factor 2. Additionally, no photons will be detected from a white dwarf above the 0.28 keV carbon K_{α} edge of the ROSAT PSPC. All other objects generally have spectra extending to higher energies.

White dwarfs with red dwarf companions are easily identified from their composite optical spectra, but for binaries with companions of spectral type K or earlier the white dwarf cannot be discerned from an optical observation (see Figure 15). However, it is possible to distinguish between the two stars with a far-UV spectrum with the IUE short wavelength (SWP) camera. Thus, initially, the stars we chose to observe with IUE were selected by the similarity of their EUV colours and luminosities to known isolated white dwarfs in the WFC survey, after the elimination of field white dwarfs in chance alignments with late-type stars, and known EUV active stars. Nine non-interacting binaries were discovered in this way and discussed by Barstow et al. (1994).

However, only a minority of stars, where the interstellar absorption is relatively low, have these characteristics. Typically the first of these systems to be identified were among the brightest EUV sources, but most isolated white dwarfs

are detected at low signal-to-noise ratio (SNR), and are indistinguishable from coronal sources from EUV data alone. Clearly, these binaries represent only part of the possible population.

Only the most active late-type stars are detected as EUV sources. Any that are weakly active must be very nearby to be seen. Thus RE J1027+323 and BD+27°1888 were included on our original IUE target list precisely because they were not known to be active. During the EUV source optical identification programme (Mason et al. 1995) observations were made of possible non-degenerate counterparts to see whether they were sufficiently active, as indicated by the strength of CaII H and K and H α emission cores, to be the EUV sources. HD2133 was listed in the WFC bright source catalogue as active, but Mason et al. (1995) found no evidence of activity and thus the most likely explanation for the EUV flux was a hidden white dwarf companion. Similarly Mullis and Bopp (1994) found that HD166435 exhibits no measurable emission in the core of H α , and could not conclude that it was chromospherically active.

RE J0357+283 was observed by Jeffries, Burleigh and Robb (1996) with the LWP camera on IUE (LWP26441) in an attempt to detect chromospheric MgII H and K emission. An excess of flux blueward of 2800Å was discovered, strongly suggesting the presence of a hot white dwarf. No MgII H and K emission was seen, and an SWP spectrum was needed to conclusively establish the presence of a white dwarf.

2.3 UV spectroscopy

A log of all the UV observations of these objects is given in Table 2. RE J1027+323 and BD+27°1888 were first observed with IUE in January 1994 as part of our original search for these systems. Repeat observations of both stars were later made to improve the quality of the data through co-addition of the spectra. HD2133 was observed in August 1995, and again in October 1995. RE J0357+283 was added to the programme and observed in August 1995 to confirm the presence of the white dwarf predicted by Jeffries, Burleigh and Robb (1996). In each case (Figures 1-5) a white dwarf is clearly identified from the blueward rising flux in the SWP spectrum. The six non-detections were all observed in this same period.

2.4 Optical spectroscopy

Optical spectroscopy of RE J1027+323, HD18131 and RE J0357+283 is reported by Genova et al. (1995), Vennes et al. (1995) and Jeffries, Burleigh and Robb (1996) respectively, and we quote their results here. BD+27°1888 was observed with the Steward Observatory 2.3m telescope on Kitt Peak, Arizona (Figure 15). We have no optical data for HD2133. Table 3 lists the parameters of the main sequence stars in the white dwarf binaries.

In Table 4 we list some of the properties of the stars observed where no white dwarf was detected. We have not observed any of these stars optically ourselves, but summarize results from other authors.

3 DATA REDUCTION

The majority of the far-UV spectra were obtained at *IUE* Vilspa. The standard IUESIPS processing was used, with the addition of the following: a white dwarf based absolute calibration including an effective area correction (Finley, 1993), and a correction for the degradation of the detector with time (Bohlin and Grillmair, 1988). Garhart (1992) used more recent *IUE* images to confirm that the degradation of the SWP camera sensitivity remained linear with time. In 1995 first Goddard, and then from October 1995 Vilspa, began using the NEWSIPS calibration which incorporates these corrections. The NEWSIPS calibrated data is indicated in Table 2. Multiple exposures were obtained for HD2133, RE J1027+322, BD+27°1888 and the ‘non-detection’ CD-44 1025, and co-added before analysis by weighting each data set according to the relative exposure times.

4 ANALYSIS

4.1 White Dwarf Binaries - UV data

In general, our analysis method follows that of Barstow et al. (1994). The *IUE* data can be used to estimate the temperature and gravity of the white dwarf by fitting the observed Lyman α profile and the uncontaminated UV continuum to synthetic white dwarf spectra. Obviously in binary systems like these, there is no possibility of fitting the Balmer line profiles in the optical region for measurement of T and log g. Unfortunately, the Lyman α information alone can give somewhat ambiguous results. For example, fitting the *IUE* SWP spectrum of the almost pure H hot white dwarf HZ43 yields T=57,500K for log g=8.5, whereas fitting the Balmer lines gives a lower T and log g of $49,000 \pm 2000$ K and 7.7 ± 0.2 (Napiwotzki et al. 1993).

We compare the observed UV data with synthetic spectra for grids of fully line blanketed LTE homogeneously mixed model atmospheres (Table 5), spanning a temperature range from 20,000K to 100,000K and log g=7.0 to 9.0, supplied by Detlev Koester (e.g. Koester 1991). The models are assumed to be pure H.

The spectral fitting is conducted with the programme XSPEC (Schafer et al. 1991), which calculates a chi-squared statistic for the fit between the data and the model, and which is then minimised by incremental steps in the free parameters. We fit the Lyman α profile and the region of the UV continuum which is uncontaminated by the primary star. Only in BD+27°1888 is there significant contamination from the companion in the SWP spectrum (Figure 4). Comparison with stars of similar spectral type (A8V-F2V) from the *IUE* archive shows that the flux is significantly greater than that of the white dwarf at $\approx 1800\text{\AA}$ but is effectively zero at 1500\AA . Thus for BD+27°1888 we fit the UV continuum up to 1500\AA . We suspected there might be a small amount of contamination in the SWP from the primary in HD2133 (Figure 1). From an *IUE* LWP spectrum (LWP31757) we estimate the spectral type of this star to be F7V-F8V. Comparison with example spectra from the *IUE* archive shows that there will be a contribution from a companion of this type of a few % of the white dwarf flux at 1800\AA , but none at 1600\AA . We therefore fit the UV continuum up to 1600\AA .

In the IUESIPS data sets, the Lyman α profile is sometimes significantly contaminated by geocoronal radiation, and only the outer wings can be used. In the NEWSIPS data, this geocoronal line is removed during the calibration process. However, we find significant differences in the fits to BD+27°1888 from the NEWSIPS and the IUESIPS data. This problem is discussed later in section 5.1.4.

There is no need to take into account any interstellar component in the fits to the Lyman α profile, because for low columns this will be negligible, and for columns of a few $\times 10^{19}$ the contribution is still lower than the typical uncertainties in the observed fluxes, between $\approx 5-10\%$. For columns greater than a few $\times 10^{19}$ the white dwarf is unlikely to be detected in EUV surveys.

The errors on the flux values are derived using the general scatter from a smooth curve passing through the SWP spectrum, since our own calibrations, unlike the NEWSIPS data, do not have an absolute error calculated for each individual data point. When the two differently calibrated data sets have been merged together, the absolute errors on the NEWSIPS data can be used to estimate the error on the co-added data.

Grids of models were determined for each star by stepping through values of log g, and finding the best fit temperature and normalisation $[(R_*/d)^2]$ at each point. The radius and mass were calculated using the evolutionary models of Wood (1995), and the radii are then used to estimate the distance from the normalisation parameter. The distances to the primaries in each case are estimated from their spectral type and V magnitude, and given in Table 3. The V magnitude of each white dwarf is estimated from the model flux at 5500\AA . These results are all given in Table 5.

4.2 White Dwarf Binaries - ROSAT data

Once the temperature and gravity of each star has been determined, the *ROSAT* EUV and soft X-ray fluxes can give an indication of the level of photospheric opacity in the white dwarf, by comparing them with predicted values for a pure H atmosphere (e.g. Barstow et al. 1993). The *ROSAT* data is fitted independently from the *IUE* data since contamination from elements heavier than H and He only has a significant effect at EUV and soft X-ray wavelengths. We fit the data from the two WFC filters, and the integrated count rate in the 0.1-0.28keV PSPC band, within which all the white dwarf soft X-ray flux is expected to lie. It is possible that some EUV and X-ray emission might originate from the main sequence star in these binaries. We therefore note the PSPC count rates at energies above 0.4keV as an indication of an active companion (Table 1).

We have fitted a set of fully line blanketed homogeneous H+He models, computed by Koester (1991), to the *ROSAT* data, again using the XSPEC spectral fitting programme. The model assumes a homogeneous distribution of H+He, under LTE conditions, in the range $-8 > \log \text{He}/\text{H} > -3$. A number of variables can determine the predicted EUV/X-ray fluxes in the model - T, log g, $[(R_*/d)^2]$, H layer mass and HI, HeI and HeII columns. A valid chi-squared analysis requires the number of degrees of freedom, ν (number of data points minus number of free parameters), to be greater than or equal to one. Since we fit only three independent data points we must use other information to specify

some of the parameters. Therefore, we use the T, log g and $[(R_*/d)^2]$, determined from the fit to the UV data and freeze these three parameters during the fit. This time, however, the He/H ratio is allowed to vary. We also make the reasonable assumption that the local ISM is not highly ionised (therefore, there is negligible HeII absorption) and that the HeI/H ratio is cosmic. Thus the HI column can be estimated.

In using this technique the χ^2 minimum is often ill-defined. We consider a good fit to the data to correspond to the probability that a particular value of the reduced χ^2 ($\chi_r^2 = \chi^2/\nu$) can occur by chance to be 0.1 or greater (i.e. 90% confidence), and a bad fit 0.01 or less (99% confidence). The fits in between may not be very good, but cannot be ruled out with high confidence. For $\nu=1$, as in this analysis, then a good fit requires χ_r^2 to be less than 2.71, but until the value of χ_r^2 exceeds 6.63 a model cannot be excluded with any certainty. We therefore note all model fits to the ROSAT data for which χ_r^2 is less than 6.63. Table 6 gives the HI column densities and He/H ratios for the homogeneous fits to the ROSAT data.

4.3 Non-detections and Active Stars

Emission features (e.g. CIV 1549Å and CII 1335Å) were detected in the IUE SWP spectra of four of the six targets where no white dwarf was seen. A search through the recent literature showed that other observers had also detected evidence for activity in these stars at optical wavelengths. We analyse the UV, EUV and soft X-ray data for these stars.

The line fluxes of the emission features were measured using a simple Gaussian profile, fitted to each line, after the continuum has first been subtracted (the continuum flux is represented by a low degree polynomial). The measured line fluxes have been compared with those of two known active stars, HD39587(χ^1 Ori, G0V) and HD126660(θ Boo, F7V), also detected by the ROSAT WFC. Low resolution SWP spectra for these stars exist in the IUE archive, and the line fluxes (Table 8) have been published by Ayres et al. (1995).

Estimates of the ratio L_{EUV}/L_{bol} have also been made as an indicator of the level of activity. We have followed the method outlined by Jeffries (1995). The S2 count rate is converted into a flux (f_{EUV}) in the 0.05-0.2 keV band using a uniform conversion rate of 1.5×10^{-10} erg cm⁻² count⁻¹, assuming an effective coronal temperature of (5-10) $\times 10^6$ K. The bolometric luminosity m_{bol} of each star is determined using the bolometric corrections given in Allen (1973). L_{EUV}/L_{bol} can then be calculated using equation (1) of Jeffries (1995). These ratios are valid assuming neutral hydrogen column densities less than $\sim 10^{19}$ cm⁻². As all four active stars lie within a few tens of parsecs of the Sun, this is a reasonable assumption.

The four active stars (CD-44 1025, HR1249, HR2468 and BD-00°1462) were also detected by the PSPC in both the soft (S, 0.1-0.4keV) and hard (H, 0.4-2.4keV) bands. We have therefore also calculated L_x and L_x/L_{bol} from the total PSPC count rate, using the hardness ratio (H-S/H+S) and the flux conversion factor given by Fleming et al. (1995). We have also calculated L_x/L_{bol} for the companion star in the WD binary HD18131, which was detected in the PSPC hard band where no flux is expected from the WD. A flux conversion factor for the hard band alone is also given by Fleming et al. (1995).

The L_{EUV}/L_{bol} and L_x/L_{bol} ratios are presented in Table 9, along with estimates of L_{EUV} and L_x .

5 DISCUSSION

5.1 White Dwarf Binaries

5.1.1 HD2133

HD2133 (Figure 1) is listed as a V=9.7 F7V star in the SIMBAD database. If these parameters are correct, it lies at a distance of ≈ 160 parsecs. If the white dwarf is associated with HD2133, then the best fit T and log g from the UV data are $26,420 \pm 500$ K and 7.50 respectively (see Table 5). However, a fit to the ROSAT data points with these parameters yields a negligible column. In fact in this direction ($l=305^\circ$, $b=-43^\circ$) and for a distance of ≈ 160 parsecs, a HI column density of $\sim 10^{19}$ cm⁻² should be expected (Diamond, Jewell and Ponman, 1995).

In the absence of optical data, we can use an IUE LWP spectrum (LWP31757) of the main sequence star to estimate its spectral type by comparing it with standard F stars in the IUE archives. Unfortunately, we could find no match in the database. We therefore suggest that we cannot be certain of the accuracy of the quoted V magnitude for this star. HD2133 would appear to be closest in flux level and spectral shape to an F8V. However, a good match to an F8V standard can only be achieved if we assume $V \approx 9.2$. This would place the star ~ 115 pc away.

At that distance, our best fit pure-H white dwarf model is log g=8.25, T $\approx 28,700$ K and M=0.79M $_{\odot}$. A corresponding fit to the ROSAT data (Table 6) gives an essentially pure H atmospheric composition, but there is still a negligible hydrogen column density. Clearly, accurate optical spectroscopy and photometry is needed to better constrain the parameters of this system.

5.1.2 HD18131

Vennes et al. (1995, hereafter V95) first reported the discovery of this binary, classifying HD18131 as K0IV, and concluded that together with the white dwarf it forms a physical pair at a distance of 70-90 pc. Based on the IUE and EUVE data sets, V95 give the white dwarf parameters as T $\approx 30,000$ K and log g ≈ 7.5 , and the interstellar column density as $\sim 10^{19}$ cm⁻². However, the PSPC count rates were not available to V95, so we include them here (Table 1).

We have adopted the same technique for analysing the IUE and ROSAT data as in the other binaries in this paper. We have no optical data for HD18131 and so we use V95's spectral classification. At a distance of 70 pc we find the white dwarf parameters are T=31,130 K, log g=8.0 and mass=0.65M $_{\odot}$ (see Table 5), giving an age for the white dwarf of ~ 10 million years. If the pair were further away at a distance of ~ 90 pc, log g=7.5, T=29,290 K and mass=0.43M $_{\odot}$, and the white dwarf is slightly younger at 7 million years. However, for log g ≥ 8.0 the temperatures given in Table 5 are considerably lower than those measured by V95 (e.g. for log g=9.0 we find T $\approx 35,000$ K but V95 give T $\approx 44,000$ K). These differences merely reflect the problems in deriving atmospheric parameters for white dwarfs from IUE data alone. The Lyman α absorption line in the SWP

spectrum of HD18131 is partly filled-in by geocornal emission (see Figure 2) and, as discussed below in Section 5.1.4, this can influence the values of the parameters measured by fitting this line. In addition, a careful comparison at the short wavelength end of the spectrum between V95's calibration and our own shows that there is a small difference of $\sim 10\%$ in the flux level at 1300Å. This may be attributable to the different method used by V95 to correct for the temporal degradation in detector sensitivity. V95 utilised an archival spectrum of the hot DA G191–B2B, a method that involves assuming appropriate atmospheric parameters for that star, whereas we have used the correction of Bohlin and Grillmair (1988).

We include only the PSPC lower band count rate (262 ± 36 counts/ks) in our analysis of the *ROSAT* data set, assuming initially that only the white dwarf is responsible for this flux. We find we can get good fits to the *ROSAT* data for $\log g = 7.5$ and 8.0 (see Table 6). At $\log g = 8.0$, the He/H ratio is $\approx 4 \times 10^{-5}$ (i.e. virtually pure hydrogen) and the interstellar hydrogen column is $7.2 \times 10^{18} \text{ cm}^{-2}$, in agreement with V95. This is the only binary in the sample in this paper that has a detection in the 0.4–2.4keV hard band of the PSPC (52 ± 16 counts/ks). Since no flux from the white dwarf is expected in this band, this soft X-ray flux must be coming from the evolved K0 companion, confirming the conclusion of V95 that the star is active. Although V95 found no CaII H & K emission cores in their optical spectrum of HD18131, the *IUE* LWP spectrum reveals Mg II emission. We derive, from the hard band count rate alone, an L_x/L_{bol} ratio of 1.4×10^{-5} , and an X-ray luminosity $L_x \approx 3 \times 10^{29} \text{ erg s}^{-1}$ (assuming $d = 70 \text{ pc}$).

Could there be a contribution from the late type star to the PSPC soft band flux? For example the white dwarf in the binary system HD217411 (Barstow et al. 1994) has a roughly similar best fit temperature ($\approx 35,600 \text{ K}$) and gravity ($\log g = 8.2$) to HD18131. The hard band count rate for this source is similar (56 ± 15 counts/ks), but there is a higher soft band rate (442 ± 38 counts/ks). The authors found they could not fit the *ROSAT* data with the parameters determined from a fit to the *IUE* data. They conclude that the G5 companion in this system is probably coronally active and contaminating the soft PSPC band.

In HD18131 we find the soft band flux can be fitted well without needing to account for a contribution from the primary. However, if we make the reasonable assumption that there is as much flux from the K0 subgiant below the carbon edge as there is above, then by subtracting this contribution (~ 50 counts/ksec) we find we can only fit the *ROSAT* data points for $\log g > 8.0$. This would set an upper limit distance to the system of ~ 70 parsecs.

5.1.3 RE J0357+283

Jeffries, Burleigh and Robb (1996, hereafter JBR96) concluded that the rapidly rotating K2 dwarf star located at the centre of the *ROSAT* source error box would have to be the most active star in the galaxy to account for all the EUV and soft X-ray flux detected by the WFC. Instead, the authors predicted that a hidden white dwarf was responsible for the EUV emission and they estimated, from the faint excess short wavelength flux in an *IUE* LWP spectrum, that any degenerate companion must have a temper-

ature between 30,000–40,000K, $\log g = 7.5–8.0$, and the H column density $N_H = (2-6) \times 10^{19}$, assuming the distance to the system to be 107pc.

An *IUE* SWP spectrum, obtained in August 1995, confirms this identification (Figure 3). If the white dwarf is associated with the K dwarf, then a fit to the UV data for $\log g = 7.9$ gives approximately the minimum distance allowed. Fits at higher gravities give distances inconsistent with that of the late-type star. At $\log g = 7.9$, the temperature of the white dwarf $T = 30,960 \text{ K}$, and $\text{mass} = 0.6 M_\odot$. Fitting the *ROSAT* data with these parameters gives $N_H = 2.1 \times 10^{19} \text{ cm}^{-2}$, and the He/H ratio $\approx 10^{-8}$. The atmosphere of this star can then be considered to be effectively pure H. We cannot fit the *ROSAT* data for $\log g < 7.9$. This source is not detected in the PSPC hard band, and JBR96 argue that the vast majority of the soft X-ray counts must be coming from the white dwarf and cannot be due to the K2V star, which shows no evidence of chromospheric Mg II emission in the *IUE* LWP spectrum.

This is the second white dwarf/rapidly rotating cool-star wide binary to be discovered. The other, BD+08°102 (RE J0044+093, Barstow et al. 1994, Kellett et al. 1995), consists of a K1–3V star with a spin period of ~ 10 hrs, and a white dwarf $T \approx 28,700 \text{ K}$, $\log g = 8.4$ and $\text{mass} \approx 0.91 M_\odot$ (distance to the system is about 55pc). The K2V primary in RE J0357+283 has an even faster rotation period of 8.76 hrs. Both JBR96 and Kellett et al. (1995) find that the binary periods of these two systems are likely to be measured in months or years, so it is unlikely that there was ever common envelope evolution to spin-up the cool stars, as is thought to have happened in the 12.5hr ‘pre-CV’ K2V/hot white dwarf binary V471 Tau (Nelson & Young 1970). Jeffries and Stevens (1996) provide an alternative model to explain the spin-up in long-period binaries. They show that a significant amount of material and angular momentum can be accreted from the slow, massive wind of an AGB star in a detached system. In this model final binary separations of up to $\sim 100 \text{ AU}$ are allowed. JBR96 also note that the cool star has a slightly enlarged radius. As the white dwarf is relatively young, ~ 8 million years in the $\log g = 7.9$ model, then this can be explained by the cool star having yet to settle at a new main sequence radius after the accretion of a large amount of mass.

5.1.4 BD+27°1888

The white dwarf companion to BD+27°1888 was discovered with *IUE* (SWP49780) in January 1994. In our initial studies of the white dwarf we utilised this spectrum because SWP49779, obtained at the same time, was overexposed in places by as much as a factor of 2. Unfortunately, the hydrogen Lyman α absorption line in SWP49780 has been heavily filled in by geocornal emission, and in addition there is a reseau mark (giving a zero reading across several channels) on one wing, making modelling extremely difficult, so we reobserved the star in the SWP and LWP cameras in November 1995. These two spectra, SWP56261 (Figure 4) and LWP31785 (Figure 12), were both extracted with the NEWSIPS calibration. In the SWP this largely removes the contamination from the geocornal Lyman α line, and thus the hydrogen absorption line can be fitted more accurately. In addition there are no zero points due to

reseau marks, and the NEWSIPS calibration also provides an absolute error for each individual data point. Figure 14 compares the NEWSIPS extracted spectrum with the earlier one, and clearly in the NEWSIPS spectrum there are many more uncontaminated data points to fit in the crucial Lyman α region. Fitting the NEWSIPS data alone, we find that the temperature is actually higher for each value of $\log g$ by $\sim 6000\text{K}$ at the lower end of the range and by $\sim 10,000\text{K}$ at the upper end. Table 7 shows a comparison between the fitted temperatures for both spectra, stepping up through $\log g$.

The differences in the fits between the two spectra is most likely due to the poor quality of the SWP49780 spectrum, in which it is necessary to remove, before modelling, a large number of the most vital data points in the Lyman α region. Therefore, rather than attempt to co-add the spectra, we decided to use the NEWSIPS calibrated spectrum alone. The results in Table 5 are all derived from this data set.

There is some discrepancy between the V magnitude given for the main sequence star in the SIMBAD database (9.6) and the Guide Star Catalogue (GSC, 9.08). We have made an estimate of V from our optical spectrum (Figure 4), and agree with the GSC value of ≈ 9.1 . Unfortunately, there was cloud during our observation and therefore the absolute flux values of the spectrum are not totally reliable. We adopt a spectral classification of A8V-F2V from this spectrum for the primary, although SIMBAD lists it as a G5. However, it is clear from Figure 4 that there is considerable flux from this star in the *IUE* SWP spectrum, where a G5 would not be seen. We also attempted to match the LWP spectrum (LWP31785) to stars of known spectral type in the *IUE* database. From this method we find the star is in fact closest in shape and flux to an A8V (Figure 12). From a quick glance through an atlas of optical spectra (e.g. Jacoby, Hunter and Christian 1984) it is immediately apparent that the differences in spectral shape between late A type stars and early Fs is very subtle. However, Figure 12 shows that at UV wavelengths the difference in flux level from one subclass to the next is substantial. In Figure 12 we compare the LWP spectrum against examples of F2V and A8V spectra from the archive, each scaled for the differences in V magnitude, and BD+27°1888 most closely resembles an A8V.

If the primary is in the range of spectral types A8-F2V and assuming $V=9.1$, it lies between 185-218 parsecs away. The closest model fit we have for a white dwarf at about that distance is $T=34,000\text{K}$, $\log g=7.25$, and $M=0.39M_{\odot}$. This mass estimate is surprisingly low, given that if this is a true binary then the white dwarf must have evolved from a progenitor more massive than an A8V. However, we must be careful not to over-interpret these results, particularly given the difficulties in fitting *IUE* data unambiguously, as discussed above. Fitting the *ROSAT* data with these parameters, we find an essentially pure H atmosphere and a column of $3.3 \times 10^{19} \text{cm}^{-2}$. The entire spectrum of BD+27°1888, from the far-UV to the optical, is displayed in Figure 15.

5.1.5 RE J1027+322

The discovery of this WD+MS binary was first reported by Genova et al. (1995, hereafter G95). The authors studied the entire field of the *ROSAT/EUVE* source, and con-

cluded that although it was more likely that the white dwarf was the sole source of the EUV flux, there may be a contribution from a QSO in the field. G95 used only a single spectrum, SWP49778, originally obtained by us in January 1994. Subsequently, we have obtained two further exposures, SWP49793 and SWP54501, and co-added all three to give the results we present here. This higher quality data allows us to better constrain the white dwarf parameters. An intense emission feature is seen in SWP49778 at 1700\AA , but there are no known strong emission features at this wavelength. G95 consider that it may well be spurious, and it is not seen in either SWP49793, taken $\approx 48\text{hrs}$ later, or in SWP54501. After examination of the photowrite image of the detector plate, we conclude that this emission feature is due to a cosmic ray hit.

G95 estimate the spectral type of the main sequence star to be G2(± 2)V, and that it lies at a distance of 380–550pc. If the white dwarf is indeed associated with this star, then we find, by fitting the *IUE* data, that it must have a surface gravity $\log g$ of 7.0-7.5 and a temperature of around 30–33,000K. However, we also find from fitting the *ROSAT* data that a good fit can only be achieved at $\log g=7.5$ or higher, although fits at $\log g=7.0$ and 7.25 cannot be completely excluded. At $\log g=7.5$, $T=32,440\text{K}$, $\log g=7.5$, $M=0.44M_{\odot}$, the column density $N_H=1.05 \times 10^{19} \text{cm}^{-2}$, and the atmosphere can be assumed to be essentially pure H.

5.2 Non-detections

5.2.1 AG+68 14

This $V=10.3$ star, listed in SIMBAD as an F8, was observed as the potential counterpart to the 2RE EUV source 0014+691. It was selected as a possible white dwarf binary on the basis that it is a very soft EUV source. The UV spectrum (Figure 6, SWP52807) shows virtually no flux above the background, except possibly at the long wavelength end. Comparing with F8 stars in the *IUE* spectral atlas (Wu et al. 1992), we would expect to see little flux from the star in the SWP camera. We conclude that there is no white dwarf companion to this star, and in the absence of any emission features in the far UV, and the non-detection of the source by the PSPC, we also conclude that it is probably not active. The field of this star needs re-examining in the optical to find the true EUV source.

5.2.2 CD-44 1025

This star is a PSPC X-ray source with a detection in the hard band ($575 \pm 41 \text{cs}^{-1}$). Early references (e.g. Malaroda 1973) claim it is a spectroscopic binary (F3V+A8V). The 2RE catalogue lists it as an F7III. Mason et al. (1995) observed the star during the WFC identification programme. They estimate the apparent EUV to optical flux ratio =2.25, and the equivalent width of the Ca H 3933 \AA chromospheric emission line $\approx 0.1\text{\AA}$. The authors note that the emission cores are variable in strength. They only class the star as an F type.

We observed the star in both the *IUE* SWP and LWP cameras (Figure 7). Our two SWP spectra (SWP56046 and SWP56047) were taken consecutively with 15 minute exposures and co-added to improve the signal/noise. Emission

lines of CIV 1549Å and HeII 1640Å are visible; measurements of these lines are presented in Table 8, where we also compare them with similar lines in low resolution *IUE* SWP spectra of HD126660 (F7V) and HD39587 (G0V), two known active stars in the WFC catalogue (RE J1425+515 and RE J0554+201).

As with BD+27°1888 (above) we attempted to match the LWP spectrum (LWP31570) to stars of known spectral type in the *IUE* archive. Figure 13 shows that at these UV wavelengths the star is closest in flux level and shape to an A8V. However, below ~2800Å the flux levels are not quite matched and this could be an indication that this is indeed a binary. In Table 9 we present measurements of the EUV and X-ray luminosities, assuming the spectral type of this star to be (a) F3V and (b) A8V.

5.2.3 HR1249

Until its discovery as an EUV source in the WFC survey, this star (RE J0402–001) was not known to be active. However, it is detected in the 0.4–2.4keV band of the PSPC, and further evidence of activity was observed optically by Mason et al. (1995) during the WFC source identification programme. They estimated the EUV to optical flux ratio=2.6, and measured the equivalent width of the CaII H 3393Å emission core=0.01Å. However, they note that they observed this weak emission core on only one occasion. The star has also been studied by Jeffries and Jewell (1993) who classify it as F6V.

Figure 8 shows SWP49792, and clearly there is no white dwarf present. However, chromospheric emission lines of CIV 1549Å, SiIV 1397Å, CII 1335Å and HeII 1640Å are visible. Measurements of these lines are presented in Table 8, and measurements of the X-ray and EUV luminosities are given in Table 9. Comparing with the known active star WFC sources HD39587 and HD126660, we conclude that HR1249 is indeed the source of the EUV radiation.

5.2.4 HR2468 (HD48189)

This star (alternatively HD48189) was not well studied prior to the WFC survey, and not known to be magnetically active. Jeffries and Jewell (1993) find it is a double star, and class the two components as G0V and K3V respectively. SIMBAD lists a combined spectral type of G1.5V. The EUV source (RE J0637–613) has proved to be a young lithium-rich object, and Jeffries (1995) measures the equivalent width of the LiI 6708Å line = 133mÅ.

The *IUE* SWP spectrum (Figure 9, SWP52802) shows no evidence for a white dwarf companion, but there are CIV 1550Å, CII 1335Å and HeII 1640Å emission lines visible. Measurements of these lines are presented in Table 8. Measurements of the EUV and X-ray luminosities in Table 9 are made assuming a G1.5V spectral classification.

5.2.5 BD-00°1462

This star was observed three times as part of the WFC optical identification programme of Mason et al. (1995), although the authors failed to find emission cores in either CaII H&K or H α , with an upper limit to the equivalent

width of 0.05Å. As an active F2V star, BD-00°1462 has been well studied in the far UV and optical (e.g. Oranje & Zwaan 1985, Simon & Landsman 1991, Andersson & Edvardsson 1994) and is very likely the optical counterpart to RE J0650–003. In the far-UV, emission cores are seen in the MgII H & K lines in high resolution LWP spectra. We obtained one low resolution SWP spectrum, SWP52801, although earlier spectra exist in the archive. Figure 10 shows the best of these, SWP8200, with an inset of SWP52801 showing a possible CIV 1549Å emission feature. There is clearly no white dwarf. This star is also an X-ray source (see Table 9).

5.2.6 HD166435

Observations of this star in the optical have revealed little evidence of activity, hence it was selected by us as a likely candidate for an unresolved white dwarf binary. The star is classified in SIMBAD as G0. Observations by Mason et al. (1995) showed it to be, at most, mildly active. They measured an equivalent width of the CaII H 3393Å emission line of 0.07Å, but detected no emission core in H α . Mullis & Bopp (1994) also concluded that there was insufficient evidence to prove that this star is chromospherically active. They found no emission core in H α , and only a small core in CaII 8542Å which they were not convinced was real.

We observed HD166435 in low resolution with the *IUE* SWP camera in August 1995 (Figure 11, SWP55658). There is clearly no white dwarf companion, and no obvious emission features although there is a hint of a CIV 1549Å emission feature rising above the background noise with a peak flux of $\sim 3 \times 10^{-14}$ ergs cm $^{-2}$ sec $^{-1}$.

The WFC source is, however, coincident with a PSPC source including a 0.4–2.4keV hard band detection. A white dwarf can be excluded as the origin of this hard band radiation, which suggests that HD166435 may indeed be coronally active. If we assume the source is HD166435, then the X-ray luminosity of this star $L_x = 9.3 \times 10^{29}$, $L_x/L_{bol} = 1.5 \times 10^{-4}$, and $L_{EUV}/L_{bol} = 1.6 \times 10^{-4}$. Comparing with the other stars in Table 9, this would make HD166435 a reasonably active object. We suggest that further high resolution optical spectroscopy of this object is required in order to unambiguously determine whether it is an active star, and the field of this source may also need re-examining.

6 SUMMARY

We have discovered three more hot white dwarfs in unresolved non-interacting binary systems with main sequence companions (HD2133, RE J0357+283 and BD+27°1888). In addition, we have independently identified a fourth system, RE J1027+322, previously reported in the literature by Genova et al. (1995). This brings the total number of such binaries found as a result of the EUV surveys to fifteen, in addition to previously identified systems also seen by the *ROSAT* WFC (e.g. V471 Tauri)*. Including WD+dM pre-

* Since this paper was first submitted, Burleigh and Barstow (1997) have discovered another WD+MS binary, RE J0500–362. This system will be discussed in more detail in a future paper.

CV and wide pairs, there are now >30 white dwarfs in non-interacting binaries that have been detected in the EUV.

Between 50 and 80% of all stars are believed to lie in binary or multiple systems. However, in the *ROSAT* X-ray catalogue of white dwarfs (Fleming et al. 1996), only 23% of the 176 objects are detected in binary systems. In addition, 75% of the ~120 *ROSAT* WFC white dwarfs appear to be single stars. It is reasonable to believe, then, that there are more white dwarf binaries in the EUV catalogues waiting to be discovered.

However, in our continuing *IUE* programme we are now observing much fainter EUV sources and less obvious candidates, and identifying new systems is becoming increasingly difficult. There are still, though, some excellent candidates to be targeted. From their WFC count rates and S2/S1 ratios it is likely that two bright EUV sources which appear to be associated with inactive B stars (HR3665 and HR2875) will have hot white dwarf companions. These white dwarfs, should they exist, will have to be identified spectroscopically with *EUVE* since the B stars will dominate the *IUE* wavelength ranges.

ACKNOWLEDGEMENTS

MRB and MAB acknowledge the support of PPARC, UK. TAF acknowledges support from NASA under grant NAGW-3160. We wish to thank Detlev Koester for the use of his white dwarf model atmosphere grids, and Jay Holberg and Jim Collins at the University of Arizona with their help in obtaining and reducing some of the data. MRB wishes to thank the staff at *IUE* Vilspa for their help and co-operation during his visits there, in particular John Fernley, Constance la Dous and Richard Monier. This research has made use of the Simbad database operated at CDS, Strasbourg, France.

REFERENCES

- Allen C., *Astrophysical Quantities*, Athlone Press, London
- Andersson H., Edvardsson B., 1994, *A&A*, 290, 590
- Ayres T.R. et al., 1995, *ApJS*, 96, 223
- Barstow M.A. et al., 1994, *MNRAS*, 270, 499
- Barstow M.A., Holberg J.B., Koester D., *MNRAS*, 1994, 270, 516
- Böhm-Vitense E., 1980, *ApJ*, 239, L79
- Böhm-Vitense E., 1993, *AJ*, 106, 1113
- Böhm-Vitense E., 1995, *AJ*, 110, 228
- Bohlin R.C., Grillmair C.J., 1988, *ApJS*, 66, 209
- Bowyer S. et al., 1994, *ApJS* 93, 569
- Bowyer S. et al., 1996, *ApJS*, 102, 129
- Burleigh M.R., Barstow M.A., 1997, in 'White Dwarfs', eds. J. Isern and M. Hernanz and E. Garcia-Berro, Kluwer, in press
- Christian D.J., Vennes S., Thorstensen J.R., Mathioudakis M., 1996, *AJ*, 112, 258
- Cooke B.A. et al., 1992, *Nature*, 355, 61
- Diamond C.J., Jewell S.J., Ponman T.J., 1995, *MNRAS*, 274, 589
- Finley D., 1993, in Proc. Conf. 'Calibrating Hubble Space Telescope', 416
- Fleming T.A., Liebert J., Green R.G., 1986, *ApJ*, 308, 176
- Fleming T.A., Schmitt J.H.M.M., Barstow M.A., Mittaz J.P.D., 1991, *A&A*, 246, L47
- Fleming T.A. et al., 1995, *ApJS*, 99, 701
- Fleming T.A., Snowden S., Pfefferman E., Briel U., Greiner J., 1996, *A&A*, 316, 147
- Garhart M., 1992, *IUE Newsletter*, No. 48, 98
- Genova R. et al., 1995, *AJ*, 110, 788
- Green R.F., Schmidt M., Liebert J., 1986, *ApJS*, 61, 305
- Hodgkin S.T., Barstow M.A., Fleming T.A., Monier R., Pye J.P., 1993, *MNRAS*, 263, 229
- Jacoby G.H., Hunter D.A., Christian C.A., 1984, *ApJS*, 56, 257
- Jeffries R.D., Jewell S.J., 1993, *MNRAS*, 264, 106
- Jeffries R.D., 1995, *MNRAS*, 273, 559
- Jeffries R.D., Burleigh M.R., Robb R.M., 1996, *A&A*, 305, L45
- Jeffries R.D., Stevens I.R., 1996, *MNRAS*, 279, 180
- Johnson H.R., Ake T.B., 1986, *ESA SP-263*, 395
- Kellett B.J. et al., 1995, *ApJ*, 438, 364
- Koester D., 1991, *IAU Symposium 145, Evolution of Stars: The Photospheric Abundance Connection*, eds. G. Michaud and A. Tutukov, Kluwer Dordrecht, 435
- de Kool M., Ritter H., 1993, *A&A*, 267, 397
- Landsman W., Simon T., Bergeron P., 1993, *PASP*, 105, 841
- Landsman W., Simon T., Bergeron P., 1996, *PASP*, 108, 250
- Liebert J., Bergeron P., Saffer R.A., 1990, *PASP*, 102, 1126
- Malaroda S., 1973, *PASP*, 85, 328
- Mason K.O. et al., 1995, *MNRAS*, 274, 1194
- Mullis C.L., Bopp B.W., 1994, *PASP*, 106, 822
- Napiwotski R. et al., 1993, *A&A*, 278, 478
- Nelson B., Young A., 1970, *PASP*, 82, 699
- Oranje B.J., Zwaan C., 1985, *A&A*, 147, 265
- Pounds K.A. et al., 1993, *MNRAS*, 260, 77
- Pye J.P. et al., 1995, *MNRAS*, 274, 1165
- Schindler M., Stencel R.E., Linsky J.L., Basri G.S., Helfand D.J., 1982, *ApJ*, 263, 269
- Schafer R.A. et al., 1991, *ESA TM-09*
- Simon T., Landsman W., 1991, *ApJ*, 380, 200
- Sims M.R. et al., 1990, *Opt. Eng.*, 29, 649
- Shipman H.L., Geczi J., in 'White Dwarfs', ed. G. Wegner, Springer-Verlag, 134
- Thompson G.I., et al., 1978, 'Catalogue of Stellar Ultraviolet Fluxes', Science Research Council, U.K.
- Trümper J., 1992, *QJRAS*, 33, 165
- Vennes S., Mathioudakis M., Doyle J.G., Thorstensen J.R., Byrne P.B., 1995, *A&A*, 299, L29
- Voges W., et al., 1997, *A&A*, in press
- Wonnacott D., Kellett B.J., Stickland D.J., 1993, *MNRAS*, 262, 277
- Wood M.A., 1995, in Proc. of the 9th European Workshop on White Dwarfs, eds. D. Koester and K. Werner, Springer, 41
- Wu C.-C. et al., 1992, *IUE Ultraviolet Spectral Atlas of Selected Astronomical Objects*, NASA Reference Publication 1285

FIGURE CAPTIONS**White Dwarf Binaries**

Figure 1. Co-added low resolution *IUE* SWP spectrum of HD2133 (SWP55659+SWP56231), compared to a predicted pure H white dwarf spectrum for $\log g=8.25$ and $T=28,700\text{K}$. Note that there may be a small contribution to the flux at the long wavelength end from the F7V–F8V companion.

Figure 2. Low resolution *IUE* SWP spectrum of HD18131 (SWP52158), compared to a predicted pure H white dwarf spectrum for $\log g=8.0$ and $T=31,130\text{K}$.

Figure 3. Low resolution *IUE* SWP spectrum of RE J0357+283 (SWP55660), compared to a predicted pure H white dwarf spectrum for $\log g=7.9$ and $T=30,960\text{K}$.

Figure 4. Low resolution *IUE* SWP spectrum of BD+27°1888 (SWP56261), compared to a predicted pure H white dwarf spectrum for $\log g=7.25$ and $T=34,130\text{K}$. Note the contribution to the flux longwards of $\sim 1600\text{\AA}$ from the A8V–F2V companion.

Figure 5. Co-added low resolution *IUE* SWP spectrum of RE J1027+322 (SWP49778+SWP49730+SWP54501), compared to a predicted pure H white dwarf spectrum for $\log g=7.5$ and $T=32,440\text{K}$.

Non-detections

Figure 6. Low resolution *IUE* SWP spectrum of AG+68 14 (SWP52807).

Figure 7. Low resolution *IUE* spectrum of CD-44 1025 (A8V–F3V, coadded SWP56046+56047 and LWP31570). Inset, the co-added SWP spectrum showing more clearly the CIV 1549Å emission feature.

Figure 8. Low resolution *IUE* SWP spectrum of HR1249 (F6V, SWP49792). Emission lines of CII 1335Å, SiIV 1397Å, CIV 1549Å and possibly HeII 1640Å are visible.

Figure 9. Low resolution *IUE* SWP spectrum of HR2468 (G1.5V, SWP52802). Emission lines of CII 1335Å, CIV 1549Å and possibly HeII 1640Å are visible.

Figure 10. Low resolution *IUE* SWP spectrum of BD-00° 1462 (F2V, SWP8210). Inset, part of SWP52801, showing a possible CIV 1549Å emission feature.

Figure 11. Low resolution *IUE* SWP spectrum of HD166435 (G0, SWP55658).

Other diagrams

Figure 12. Low resolution *IUE* LWP spectrum of BD+27° 1888 (LWP31785, solid line) and comparison spectra - HD28910 (LWP27455, A8V, dashed line) and HD29875 (LWP20865, F2V, dotted line), scaled for differences in magnitude (assuming $V=9.1$ for BD+27° 1888).

Figure 13. *IUE* LWP spectrum of CD-44 1025 (LWP31570, solid line) and comparison spectrum - HD28910 (LWP27455, A8V, dashed line), scaled for difference in magnitude.

Figure 14. Comparison of NEWSIPS SWP spectrum of BD+27° 1888 (SWP56261, upper) with the older IUESIPS-extracted SWP49780 (lower). The flux levels are arbitrary. Note the presence of a strong geocoronal Lyman α emission line in SWP49780.

Figure 15. *IUE* SWP and LWP spectra of BD+27°1888 (WD+F2V), displayed together with an optical spectrum and a pure H model white dwarf spectrum for $T=34,130\text{K}$ and $\log g=7.25$. The white dwarf can be seen emerging from the glare of its companion shortwards of $\sim 1600\text{\AA}$. This diagram clearly illustrates that the white dwarfs in these binaries are undetectable at optical wavelengths and can only be seen in the far-UV.

Figure 1 HD2133 IUE SWP

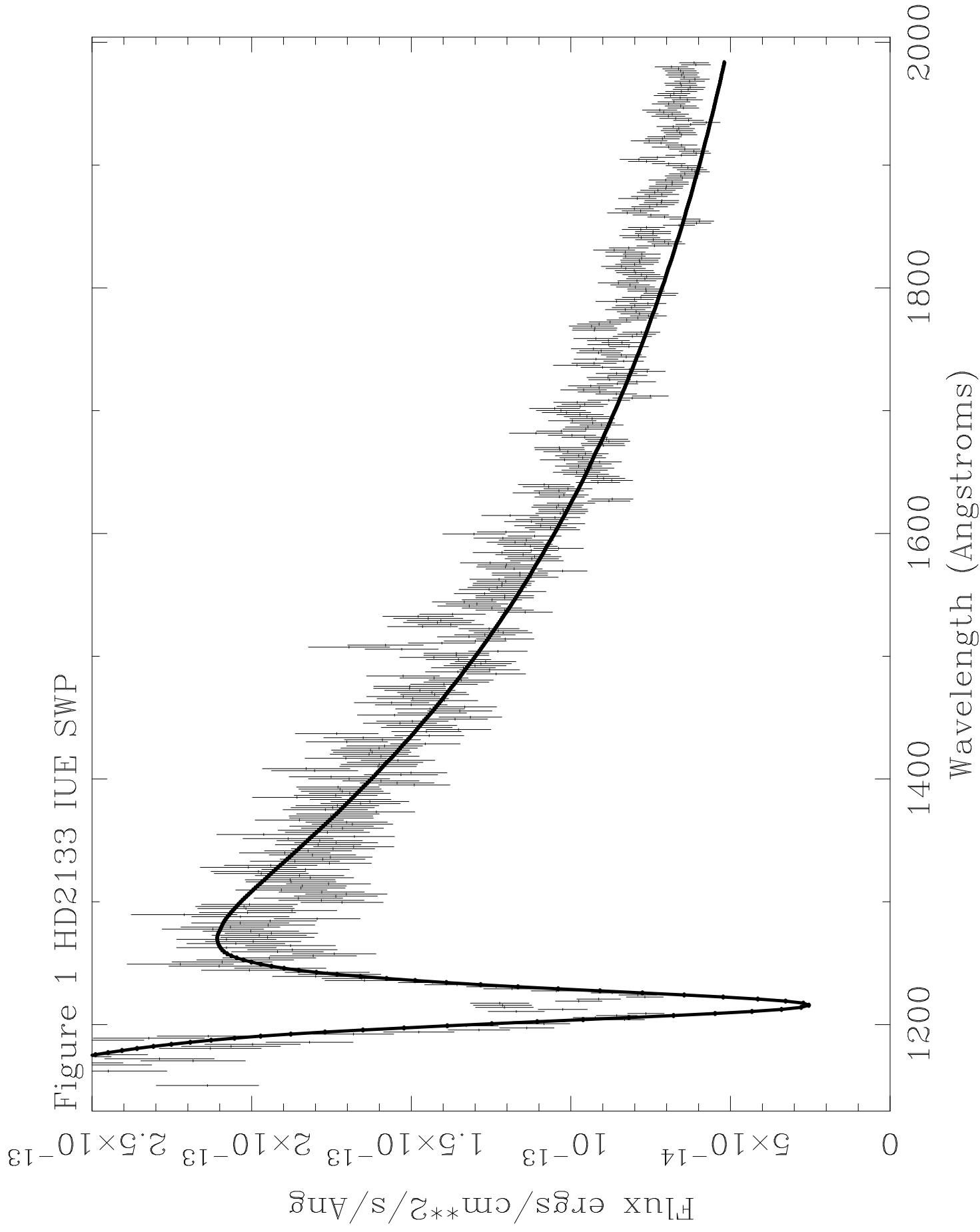


Figure 2 HD18131 IUE SWP

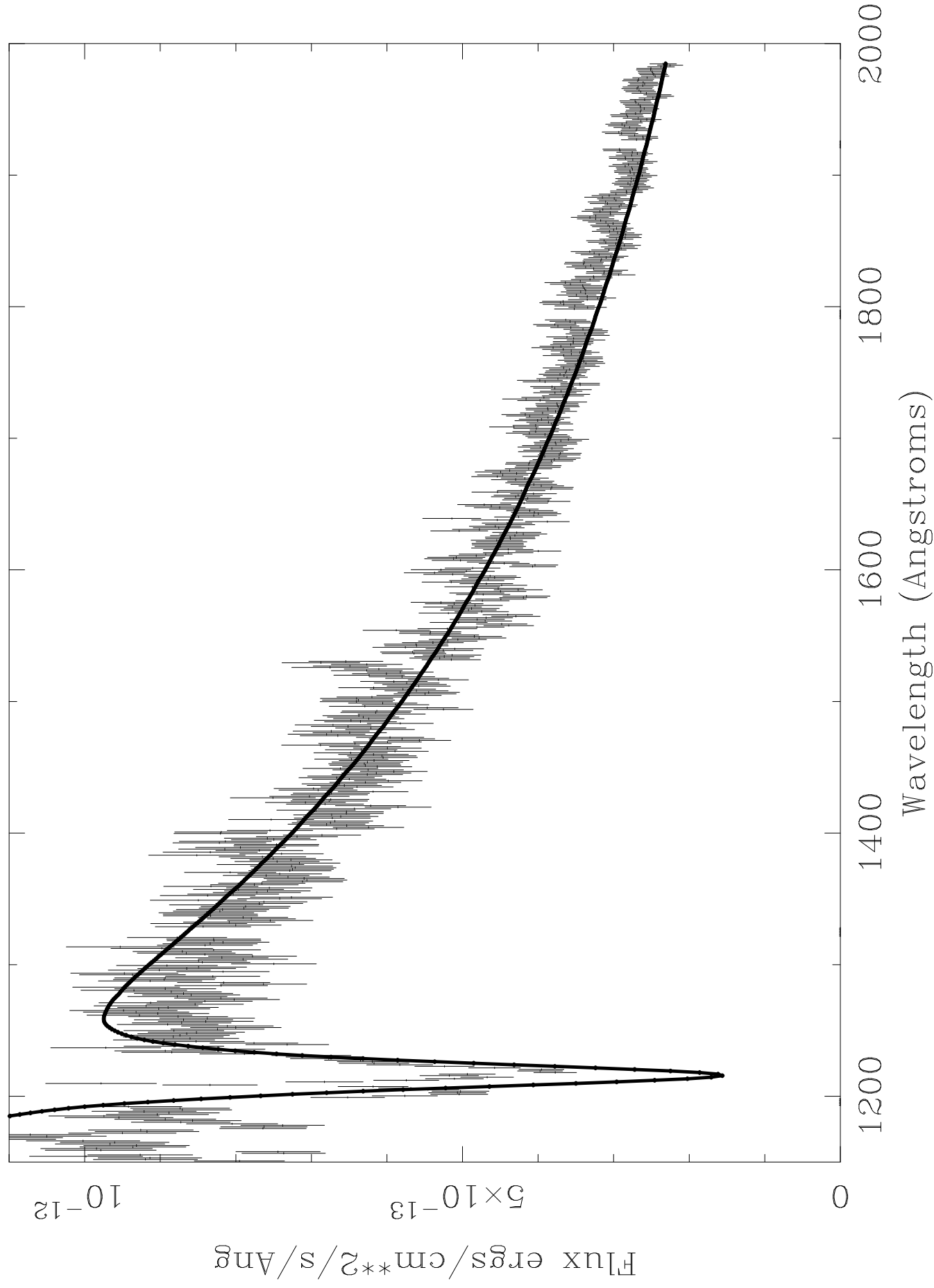


Figure 3 RE J0357+283 IUE SWP

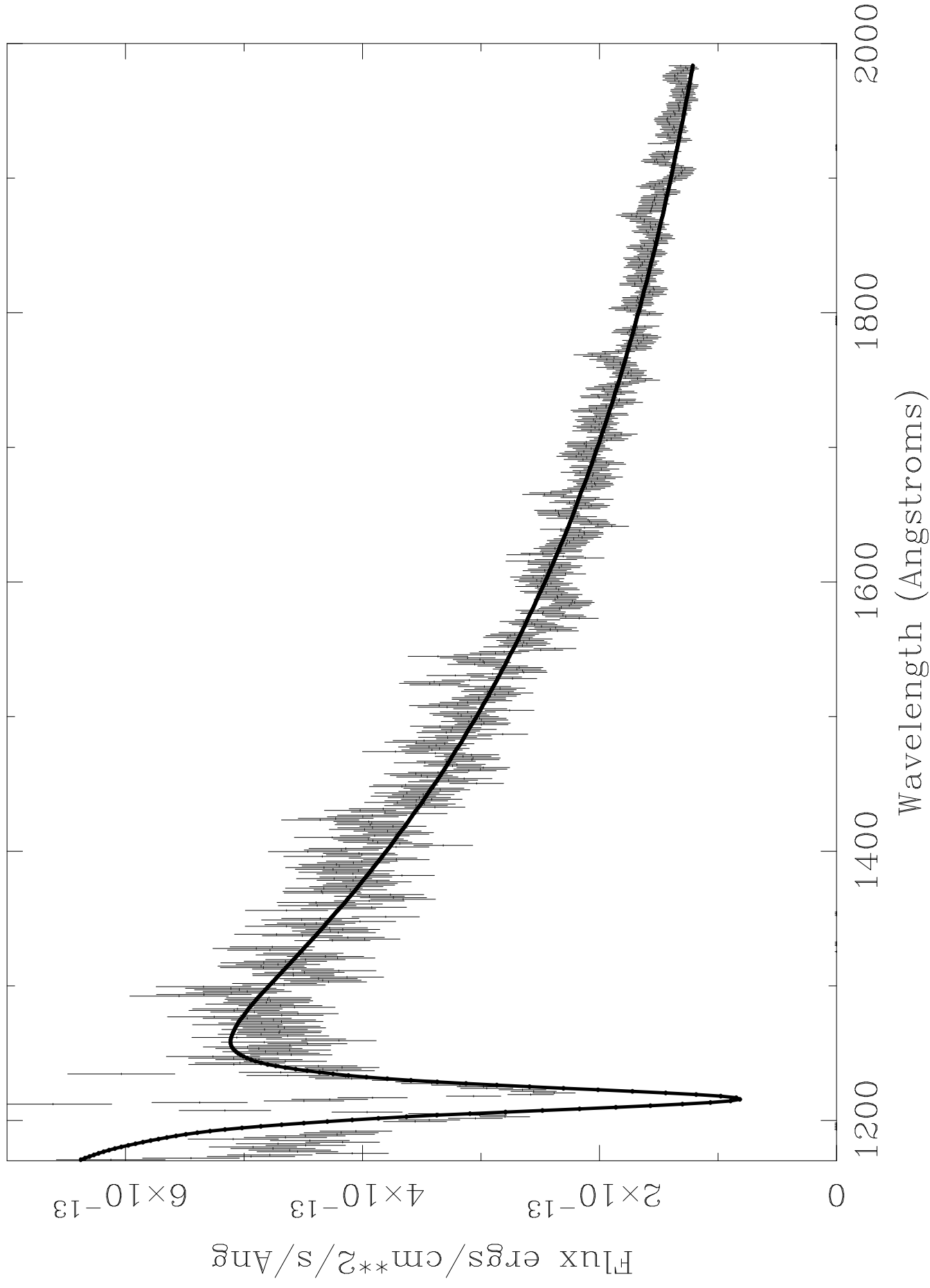


Figure 4 BD+27 1888 IUE SWP

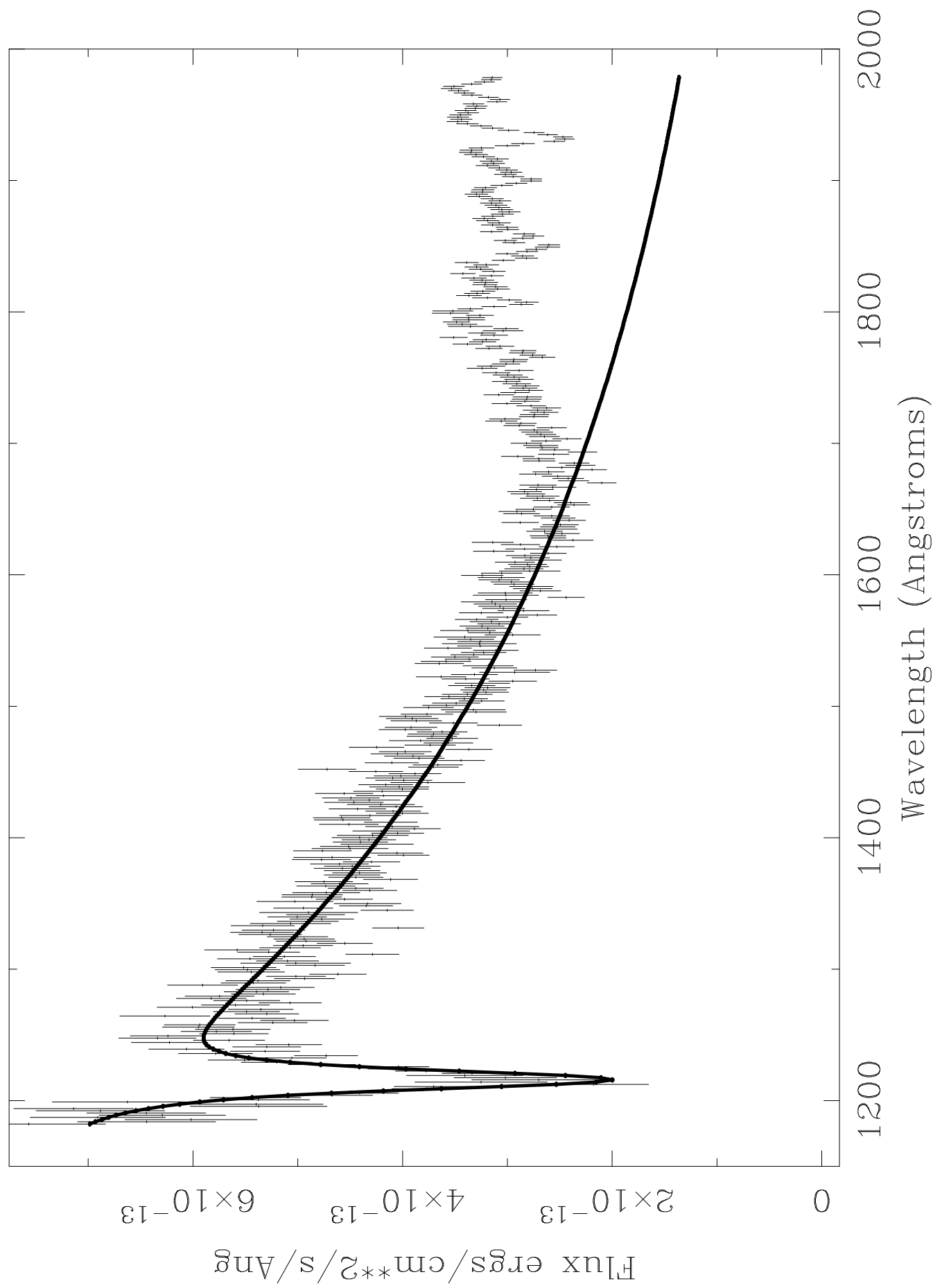


Figure 5 RE J1027+322 IUE SWP

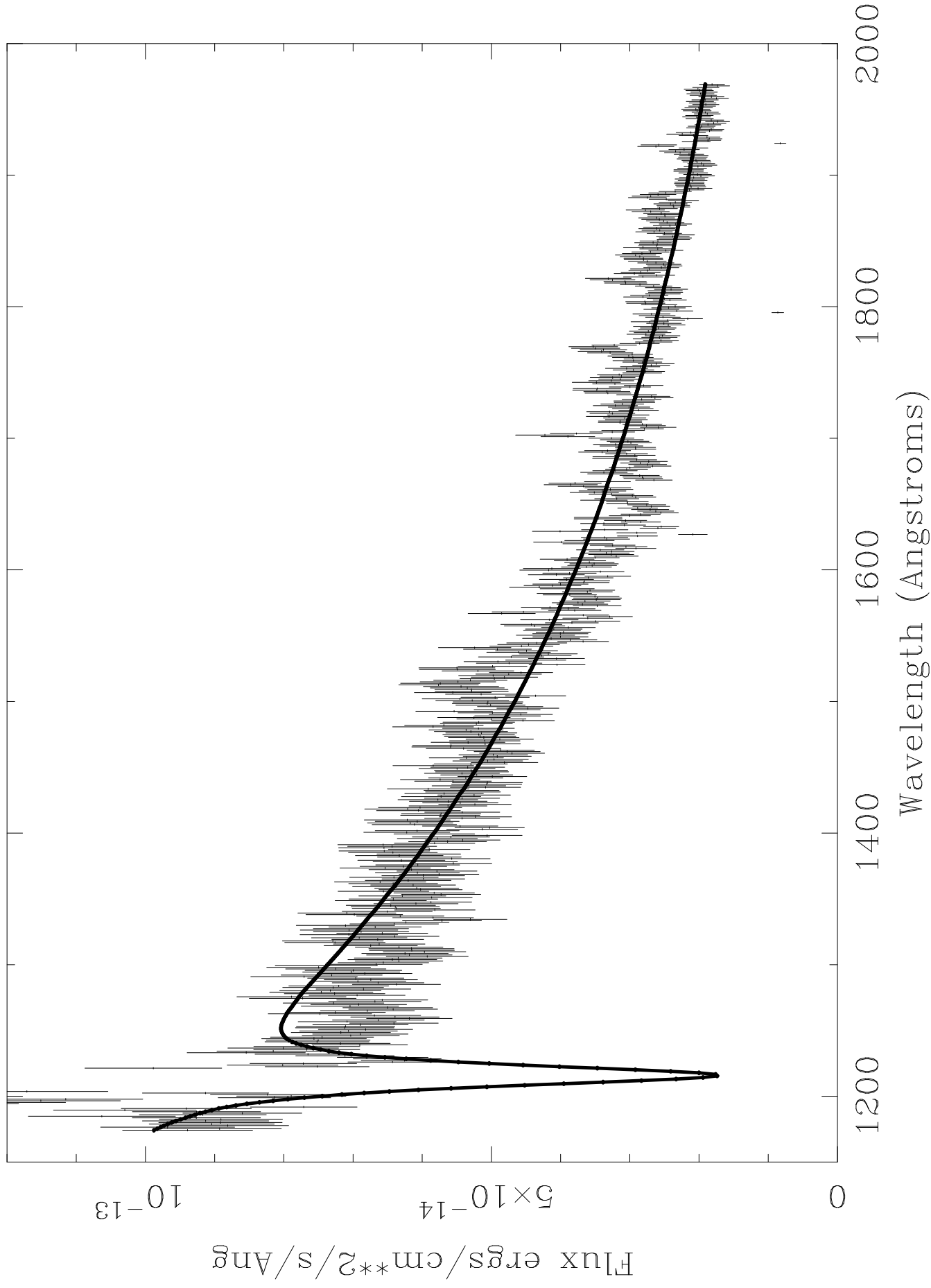


Figure 6 AG+68 14 IUE SWP

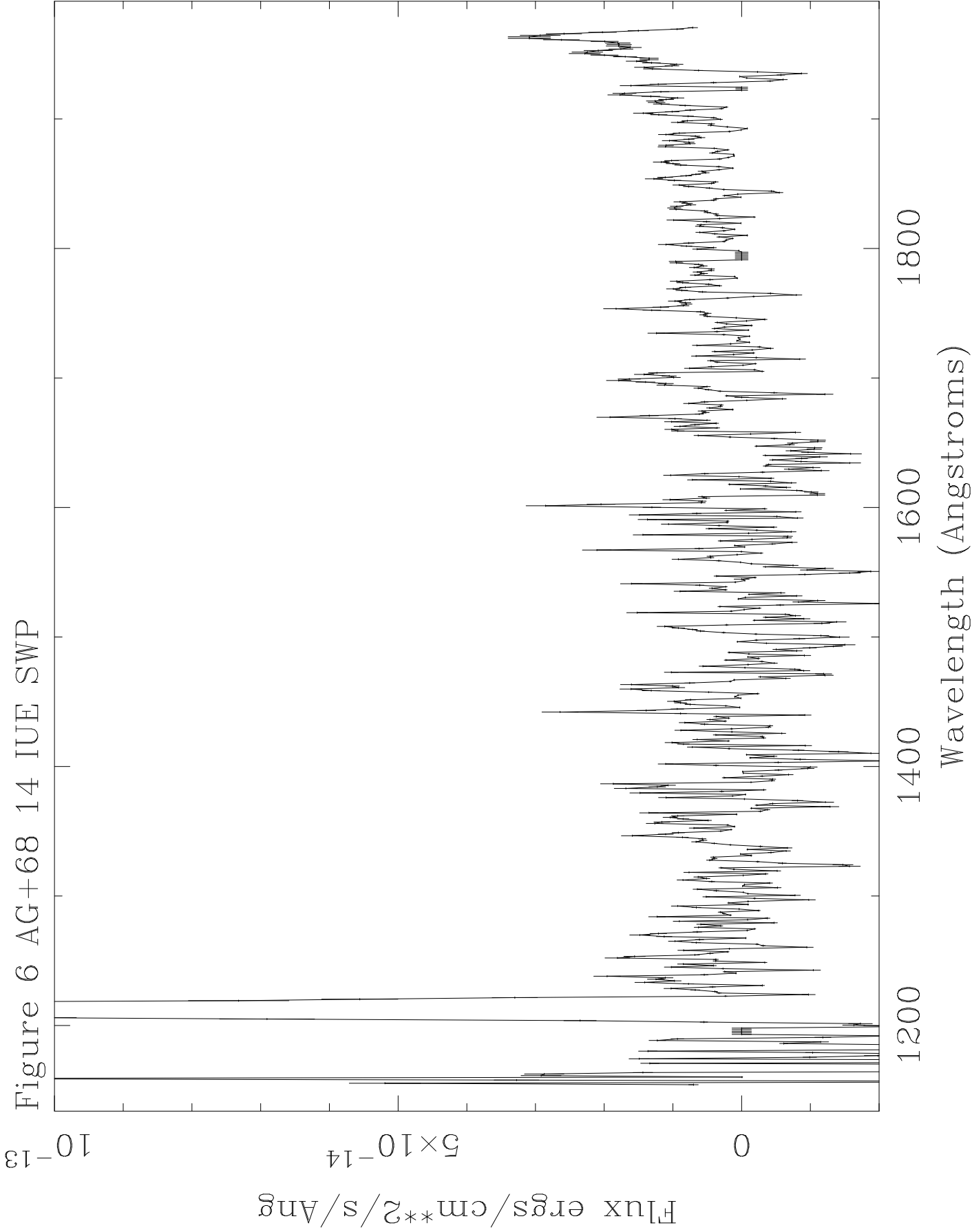


Figure 7 CD-44 1025 IUF SWP+LWP

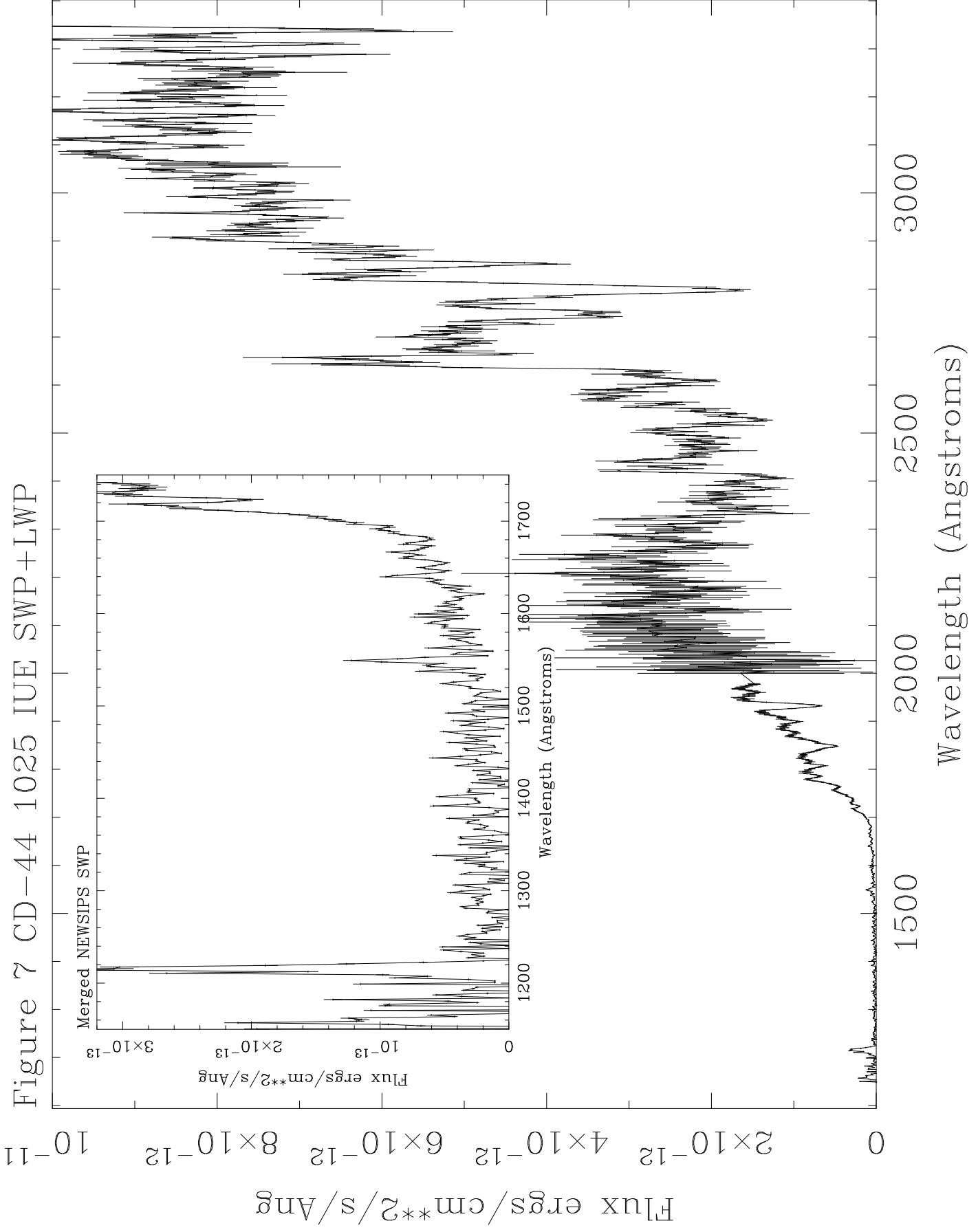


Figure 8 HR1249 IUE SWP

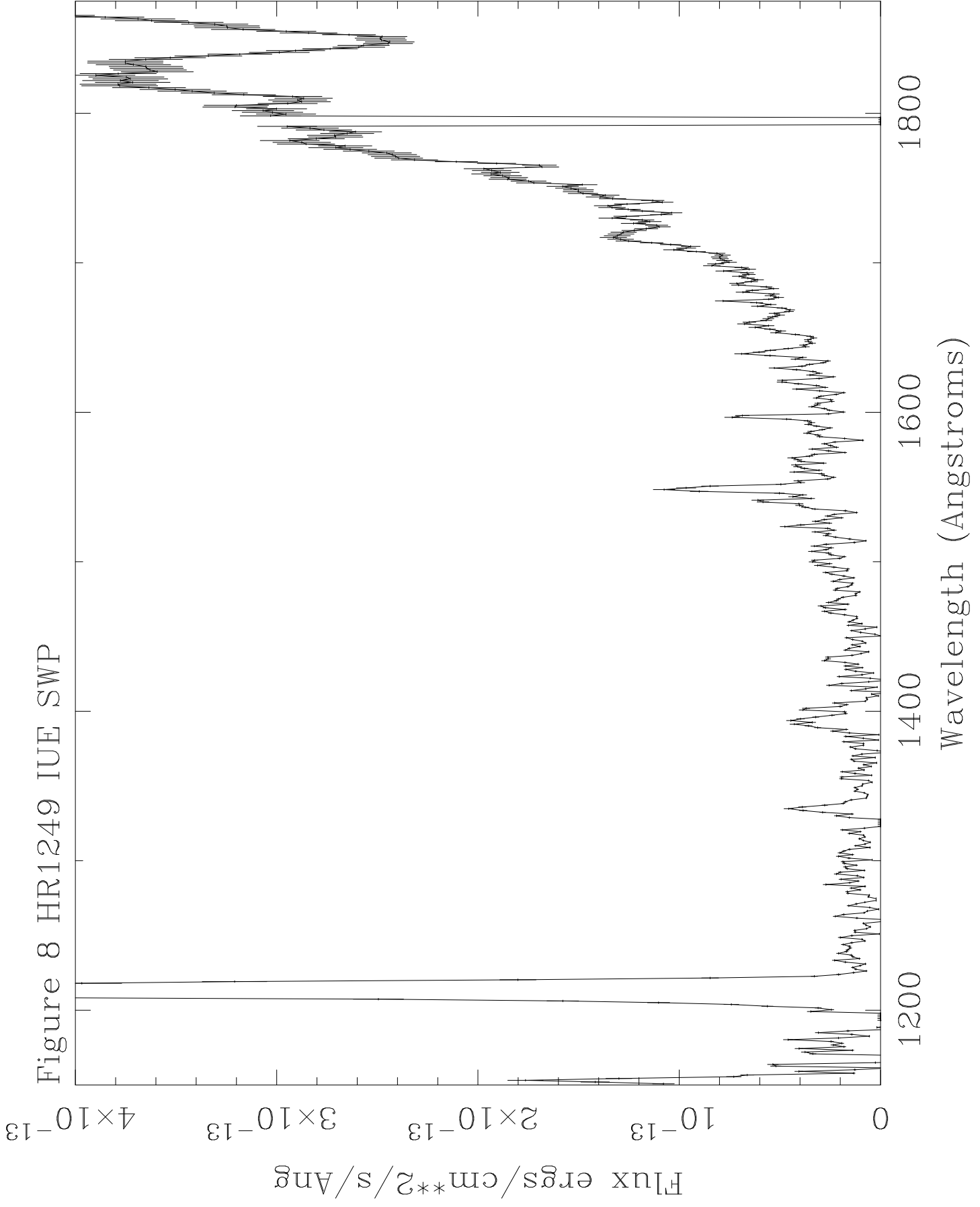


Figure 9 HR2468 IUE SWP

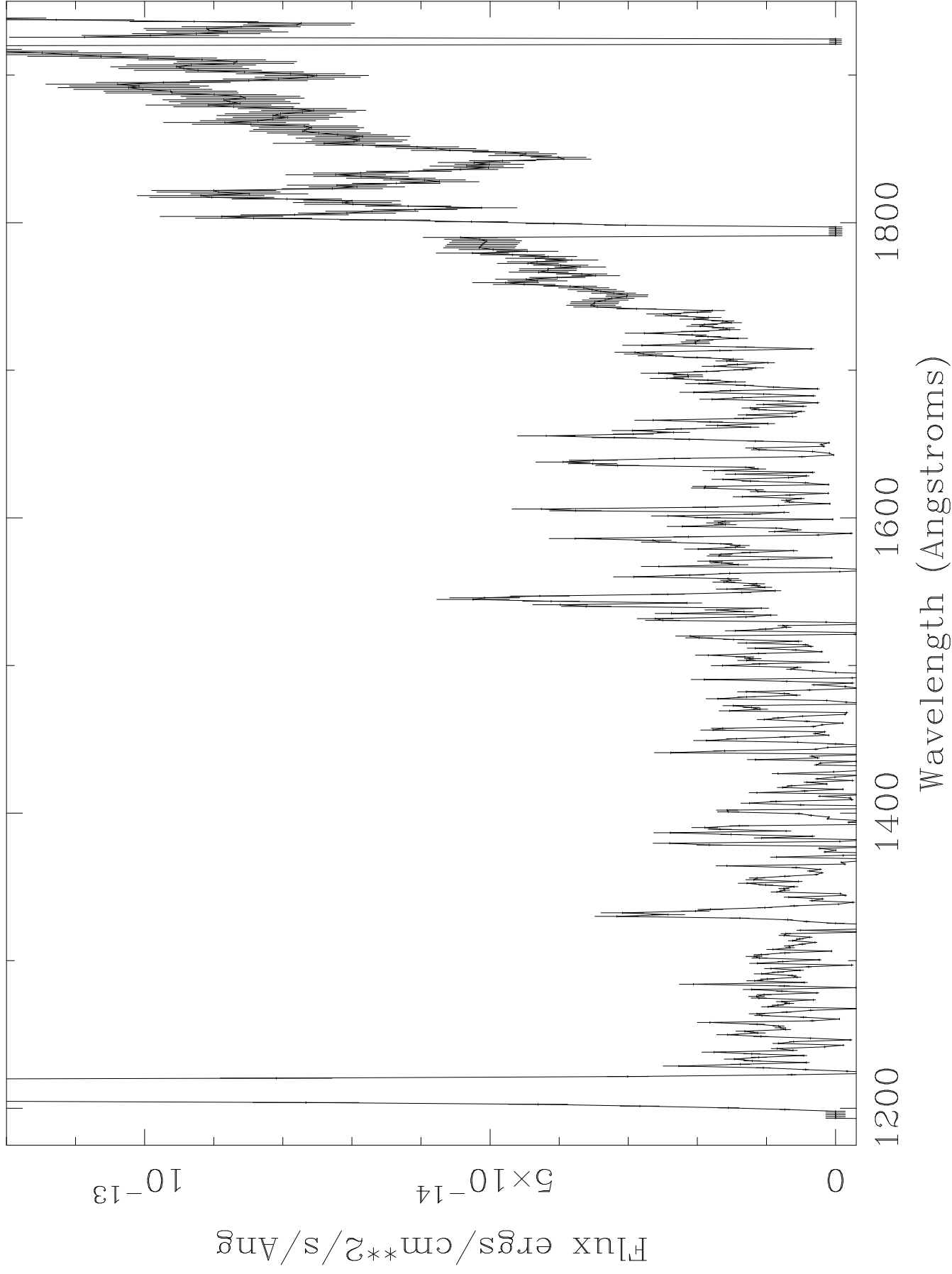


Figure 10 BD-00 1462 IUE (SWP8200)

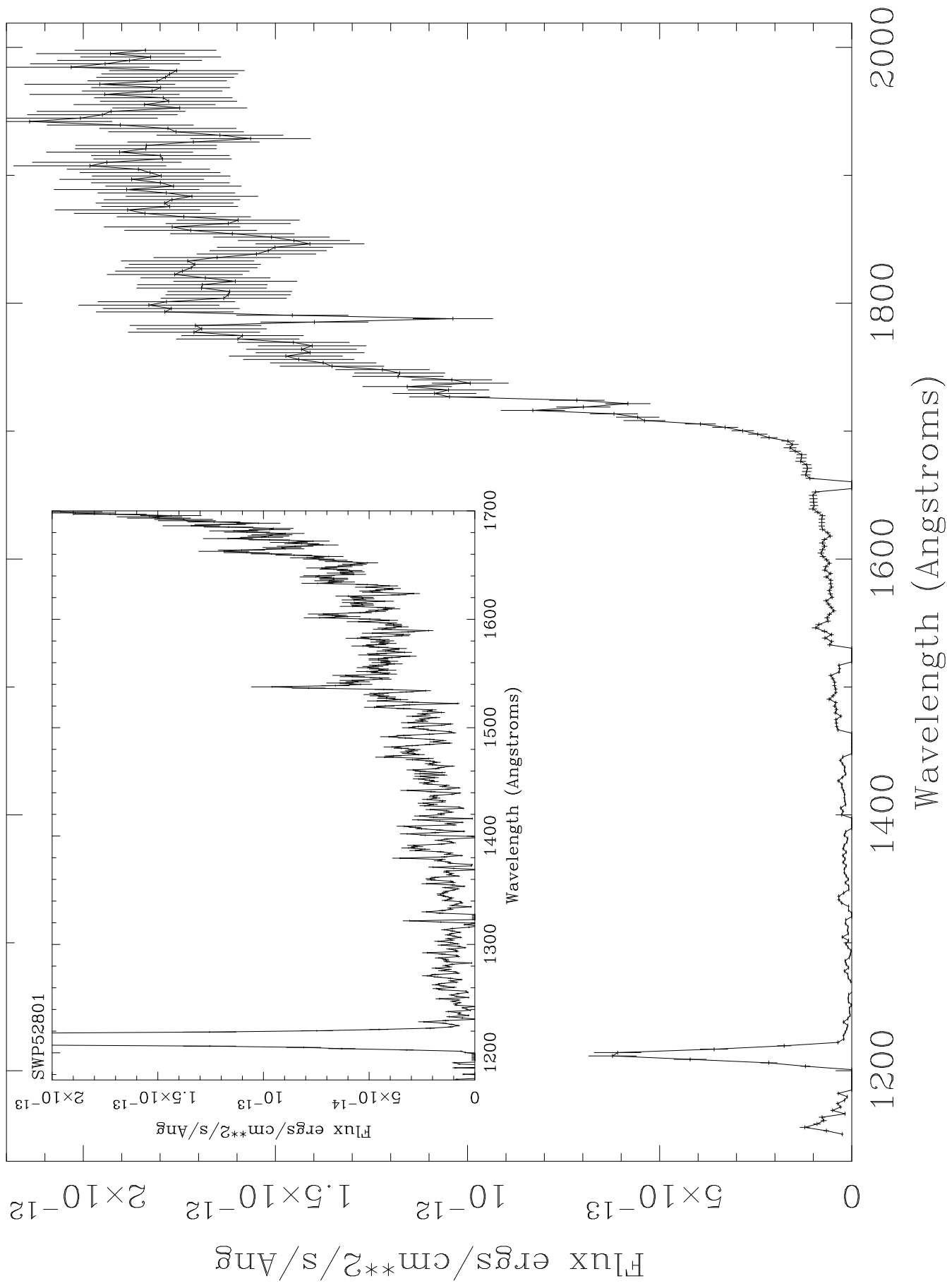


Figure 11 HD166435 IUE SWP

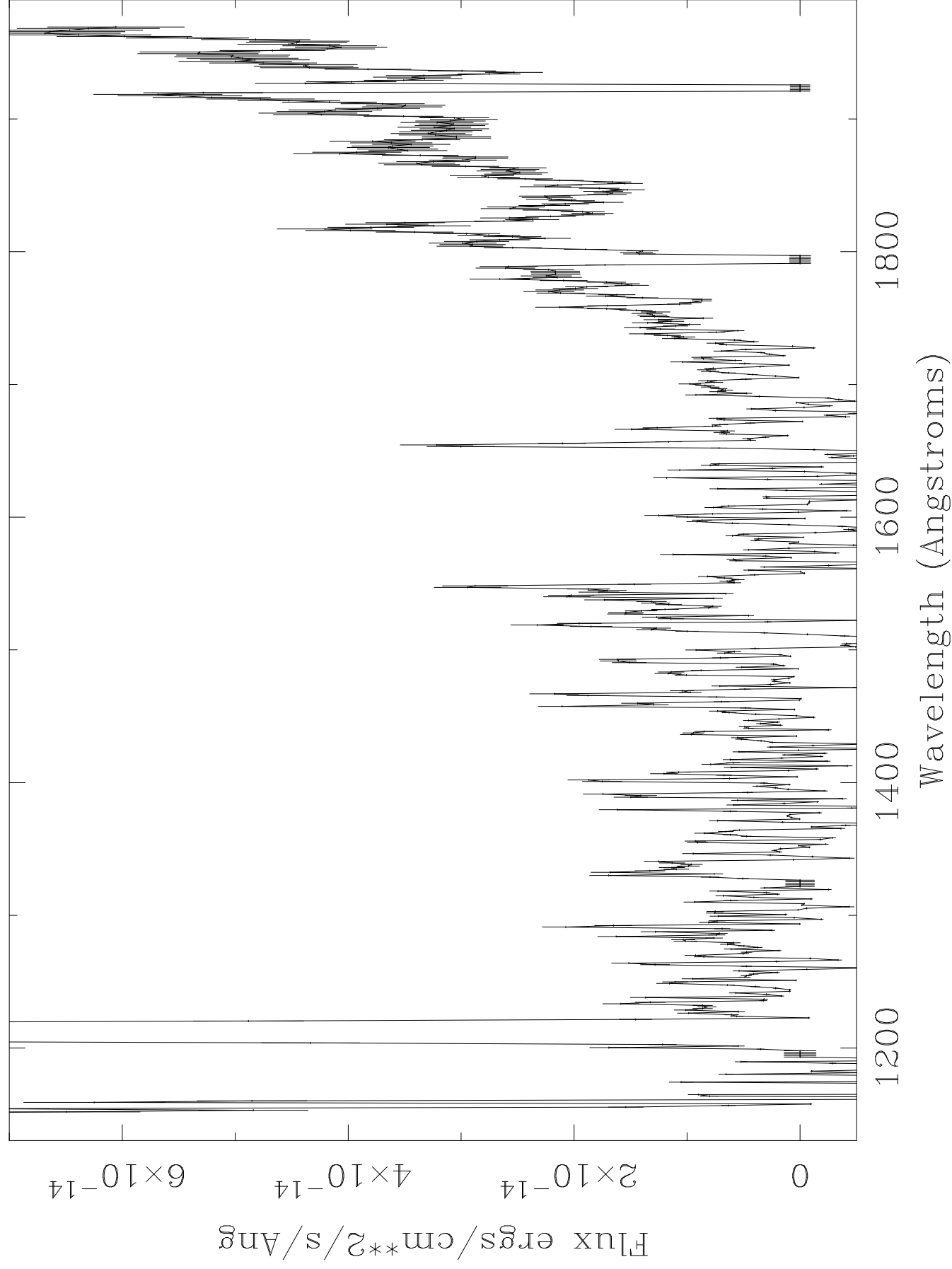


Figure 12 BD+27 1888 LWP and comparison spectra

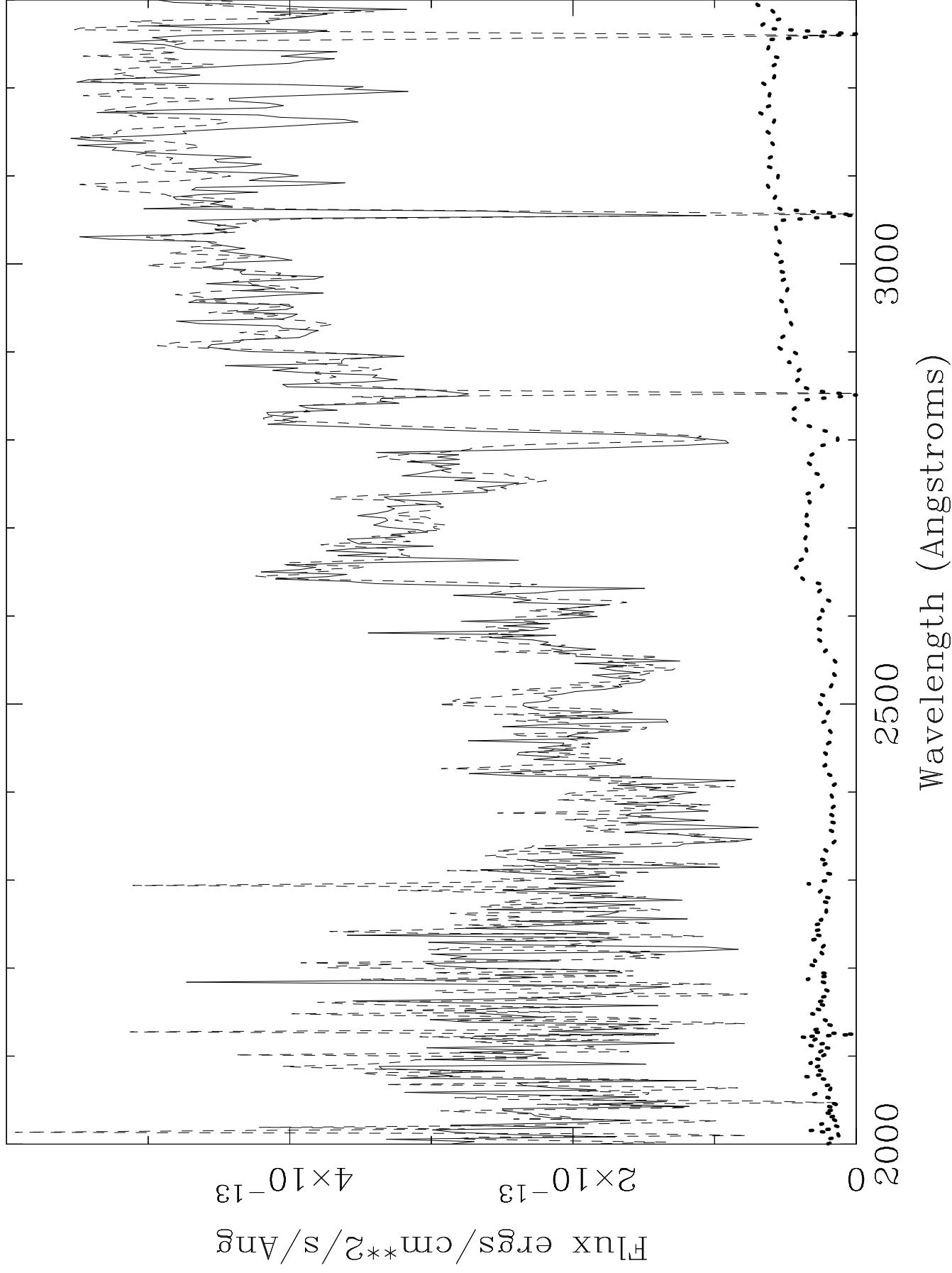


Figure 13 CD-44 1025 IUE LWP and A8V comparison spectrum

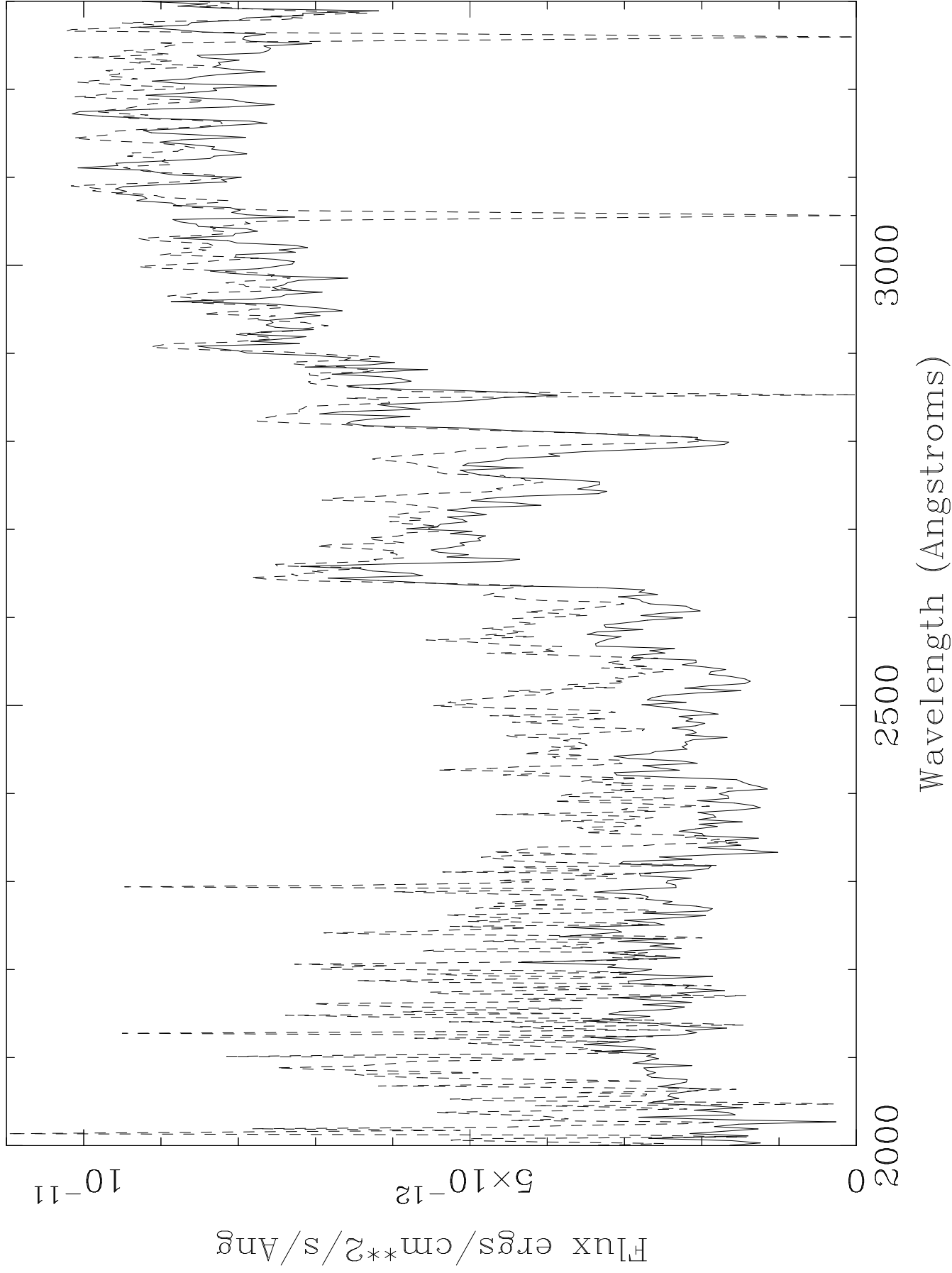


Figure 14 BD+27 1888 IUESIPS (lower) and NEWSIPS (upper)

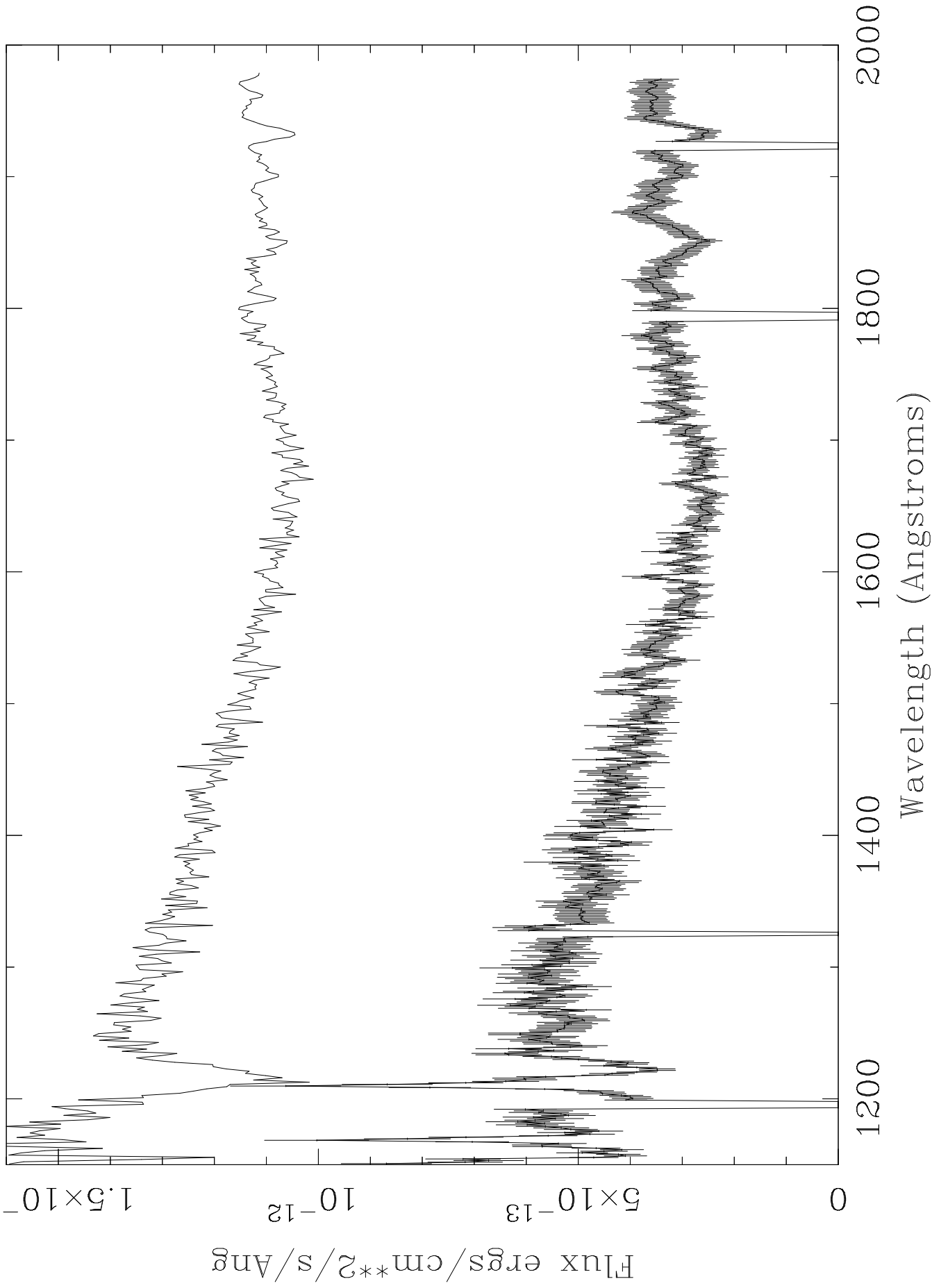


Figure 15 BD+27 1888 IUE SWP+LWP+Optical and WD model

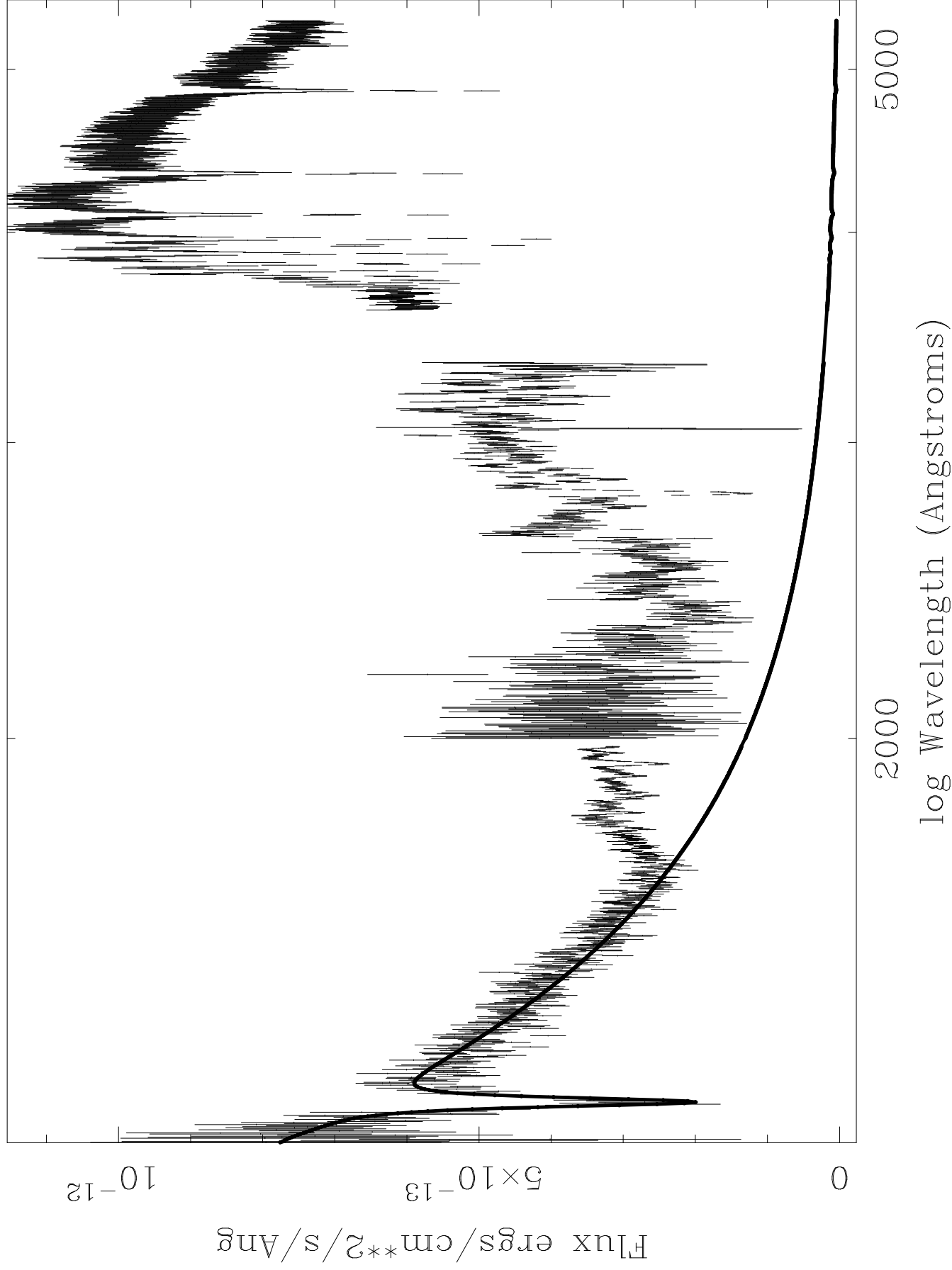


Table 1. ROSAT WFC/PSPC and EUVE count rates (1000s⁻¹)

Name	WFC		PSPC		EUVE	
	S1	S2	(0.1-0.4keV)	(0.4-2.4keV)	100Å	200Å
WD Binaries						
HD2133	14±5	32±9	46±11	no det.	no det.	no det.
HD18131	65±13	127±21	262±36	52±16	137±14	44±12
RE J0357+283	46±9	55±10	210±29	no det.	54±11	no det.
BD+27°1888	33±5	19±7	212±24	no det.	46±10	no det.
RE J1027+323	15±4	23±7	52±17	no det.	40*	no det.
Non-WD Systems						
2RE J0014+69 ¹	no det.	36±10	no det.	no det.	no det.	no det.
CD-44 1025	25±6	27±6	693±47	575±41	36±7	no det.
HR1249	34±6	41±7	785±50	739±48	50±12	no det.
HR2468	34±3	32±4	1389±38	919±31	47±4	9±4
BD-00°1462	13±3	26 [†]	196±28	134±22	no det.	no det.
RE J1809+29 ²	26±4	51±13	307±21	197±17	25±7	no det.

* No error given in Bowyer et al. (1996), [†] upper limit

1] AG+68 14 was observed as a possible counterpart to this source

2] HD166435 was observed as a possible counterpart to this source

Table 2. Log of IUE observations

Name	IUE SWP No.	LWP No.	Date	Exposure (s)	Observer	notes
WD Binaries						
HD2133	55659		1995/234	1800	Burleigh	
	56231		1995/329	2700	SO	newsips
		31757	1995/329	600	SO	newsips
HD18131	52151		1994/266	5500	Vennes	mildly saturated
	52158		1994/267	2000	Byrne	
RE J0357+283	55660		1995/234	3780	Burleigh	
		26441	1993/265	1500	Jeffries	
BD+27°1888	49779		1994/006	4000	Burleigh	2× over-exposed
	49780		1994/006	1200	Burleigh	
	56261		1995/336	1200	SO	newsips
		31785	1995/336	300	SO	newsips
RE J1027+322	49778		1994/006	1200	Burleigh	
	49793		1994/008	11100	Burleigh	
	54501		1995/115	7500	Burleigh	newsips
Non-WD Systems						
AG+68 14	52807		1994/319	1800	Burleigh	
CD-44 1025	56046		1995/274	900	SO	newsips
	56047		1995/274	900	SO	newsips
		31570	1995/274	35	SO	newsips
HR1249	49792		1994/008	2400	Burleigh	
HR2468	52802		1994/318	1800	Burleigh	
BD-00°1462	8200		1980/069	3000	Oranje	
	52801		1994/318	1800	Burleigh	
HD166435	55658		1995/264	3600	Burleigh	

SO=Service Observation

Table 3. Physical parameters of the companion stars in the binaries

RE No.	Cat. Name	Spectral type	V magnitude	d est. (pc)	references
RE J0024-741	HD2133	F8V	9.7	146	
RE J0254-053	HD18131	K0IV	7.32	67	1
RE J0357+283		K2V	11.7	>107	2
RE J1024+262	BD+27°1888	A8V-F2V	9.1	185-218	
RE J1027+322		G2(\pm 2)V	13.0	380-550	3

Refs. 1] Vennes et al. (1995) 2] Jeffries, Burleigh & Robb (1996) 3]Genova et al. (1995)

Table 4. Physical parameters of the stars observed where no white dwarf was detected

RE No.	Cat. Name	Spectral type	V magnitude	references
2RE J0014+691	AG+68 14	F8	10.3	simbad
RE J0312-442	CD-44 1025	F3V+A8V	5.93	simbad
RE J0402-001	HR1249	F6V	5.38	simbad
RE J0637-613	HR2468	G1.5V	6.18	simbad
RE J0650-003	BD-00°1462	F2V	5.77	simbad
RE J1809+295	HD166435	G0	6.84	simbad

Table 5. Temperatures and gravities for the white dwarfs from homogeneous model fits

Binary	log g	Temp K	90% error K	Mass M_{\odot}	Radius R_{\odot}	d _{wd} (pc)	Estimated V
HD2133	7.0	24,490	24,160-24,870	0.37	0.032	234	15.4
	7.5	26,420	26,100-26,810	0.42	0.019	165	15.6
	7.75	26,780	26,510-27,270	0.52	0.016	139	15.6
	8.0	28,260	27,910-28,630	0.65	0.013	132	15.7
	8.25	28,700	28,350-29,050	0.79	0.011	112	15.7
	8.5	29,900	29,560-30,400	0.95	0.009	100	15.8
	9.0	31,650	31,240-32,260	1.20	0.006	68	15.9
HD18131	7.0	26,440	26,170-26,740	0.37	0.032	126	13.9
	7.5	29,290	28,650-29,640	0.43	0.019	93	14.1
	8.0	31,130	30,750-31,540	0.65	0.013	72	14.2
	8.5	32,980	32,530-33,470	0.95	0.009	53	14.2
	9.0	35,050	34,500-35,640	1.20	0.005	36	14.3
RE J0357+28	7.0	27,330	27,050-27,640	0.37	0.032	185	14.6
	7.5	29,460	29,130-29,820	0.43	0.019	130	14.8
	7.9	30,960	30,620-31,410	0.60	0.014	105	14.9
	8.0	31,340	30,940-31,760	0.65	0.013	100	14.9
	8.5	33,430	32,950-33,950	0.95	0.009	75	14.9
	9.0	35,840	35,240-36,540	1.20	0.005	51	15.0
BD+27°1888	7.0	33,180	32,340-34,380	0.38	0.032	242	14.8
	7.25	34,130	33,330-35,780	0.39	0.025	193	14.8
	7.5	35,370	34,530-37,300	0.45	0.020	162	14.9
	8.0	38,420	37,330-40,870	0.67	0.014	120	14.9
	8.5	42,470	41,050-45,690	0.96	0.009	89	15.0
	9.0	47,640	45,800-51,790	1.21	0.005	61	15.1
RE J1027+32	7.0	30,560	29,560-32,600	0.37	0.032	589	16.9
	7.25	32,265	30,760-33,500	0.39	0.025	487	16.9
	7.5	32,440	31,570-34,450	0.44	0.020	388	16.9
	8.0	34,000	33,400-36,460	0.66	0.013	288	17.0
	8.5	37,020	35,620-38,650	0.96	0.009	216	17.1
	9.0	39,240	37,910-41,380	1.20	0.005	144	17.2

Table 6. He/H ratios and column densities from homogeneous models

Name	log g	T	He/H	HI column	χ_r^2	Comment
HD2133	7.0	24,490	-	-	19.2	No Fit
	7.5	26,420	1×10^{-8}	0.0	2.71	
	7.75	26,780	1.35×10^{-7}	0.0	0.79	
	8.0	28,260	1.29×10^{-5}	1.58×10^{18}	0.54	
	8.25	28,700	3.00×10^{-5}	0.0	0.63	
	8.5	29,900	5.89×10^{-5}	0.0	1.56	
	9.0	31,460	-	-	8.44	No Fit
HD18131	7.0	26,440	-	-	17.0	No Fit
	7.5	29,290	1×10^{-8}	1.17×10^{19}	1.61	
	8.0	31,130	3.63×10^{-5}	7.20×10^{18}	1.17	
	8.5	32,980	2.29×10^{-4}	0.0	3.64	
	9.0	35,050	4.90×10^{-3}	0.0	2.31	
RE J0357+283	7.0	27,330	-	-	22.9	No Fit
	7.5	29,460	-	-	11.4	No Fit
	7.9	30,960	6.67×10^{-5}	2.10×10^{19}	4.27	
	8.0	31,340	6.90×10^{-5}	2.27×10^{19}	3.16	
	8.5	33,430	7.33×10^{-5}	1.92×10^{19}	2.08	
	9.0	35,840	6.91×10^{-5}	1.02×10^{19}	2.42	
BD+27°1888	7.0	33,180	-	-	17.5	No Fit
	7.25	34,130	9.8×10^{-7}	3.31×10^{19}	3.28	
	7.5	35,370	1×10^{-8}	4.79×10^{19}	3.87	
	8.0	38,420	1×10^{-8}	7.25×10^{19}	6.27	
	8.5	42,470	-	-	22.7	No Fit
	9.0	47,640	-	-	31.0	No Fit
RE J1027+323	7.0	30,560	1.0×10^{-8}	2.86×10^{18}	5.85	
	7.25	32,265	9.55×10^{-7}	8.24×10^{18}	3.31	
	7.5	32,440	4.78×10^{-7}	1.05×10^{19}	2.38	
	8.0	34,000	1.0×10^{-8}	1.66×10^{19}	1.25	
	8.5	37,020	2.51×10^{-4}	0.0	2.04	
	9.0	39,240	5.75×10^{-4}	0.0	3.24	

Table 7. BD+27°1888: Comparison between the temperatures derived from fitting SWP49780 and SWP56261 (NEWSIPS)

log g	SWP49780		SWP56261	
	Temp	90% Range	Temp	90% Range
7.0	27,620	26,760-29,140	33,180	32,340-34,380
7.5	30,400	29,220-31,470	35,370	34,530-37,300
8.0	31,980	31,000-33,480	38,420	37,330-40,870
8.5	34,390	33,080-35,865	42,470	41,050-45,690
9.0	37,180	35,615-38,740	47,640	45,800-51,790

Table 8. Line fluxes for the active stars observed with IUE

Name	CII*	SiIV*	CIV*	HeII*
	1335Å	1397Å	1549Å	1640Å
HD39587 ⁺	4.02±0.12	4.01± 0.14	5.15±0.14	2.50±0.11
HD126660 ⁺	6.21±0.5	4.74±0.34	10.4±0.62	2.91±0.5
CD-44 1025	-	-	4.40±0.67	1.35±0.40
HR1249	1.83±0.24	3.67±0.43	4.11±0.35	0.75±0.21
HR2468	1.26±0.22	-	2.89±0.4	1.26±0.29
BD-00°1462	-	-	1.82±0.34 [†]	-

* $\times 10^{-13}$ ergs/cm²/sec, ⁺ comparison star (see text), [†] possible detection

Table 9. EUV and X-ray luminosities for the active stars observed

Name	d(pc)	L_{EUV} $\times 10^{29}$ ergs	L_{EUV}/L_{bol} $\times 10^{-5}$	L_x $\times 10^{29}$ ergs	L_x/L_{bol} $\times 10^{-5}$
HD39587 ⁺	11	0.8	1.2	1.9	3.0
HD126660 ⁺	12	0.9	0.8	2.9	2.8
CD-44 1025(F3V)	37	6.6	3.8	16.7	9.6
CD-44 1025(A8V)	51	12.6	3.5	31.7	8.8
HR1249	23	3.9	3.5	7.9	7.1
HR2468	23	3.0	5.5	10.9	19.7
BD-00°1462	36	6.0 [†]	3.1 [†]	3.8	2.0

⁺ comparison star (see text), [†] upper limit